Ultrasound of the Liver
Benign Liver Lesions

Deike Strobel
University Hospital Erlangen (Germany)

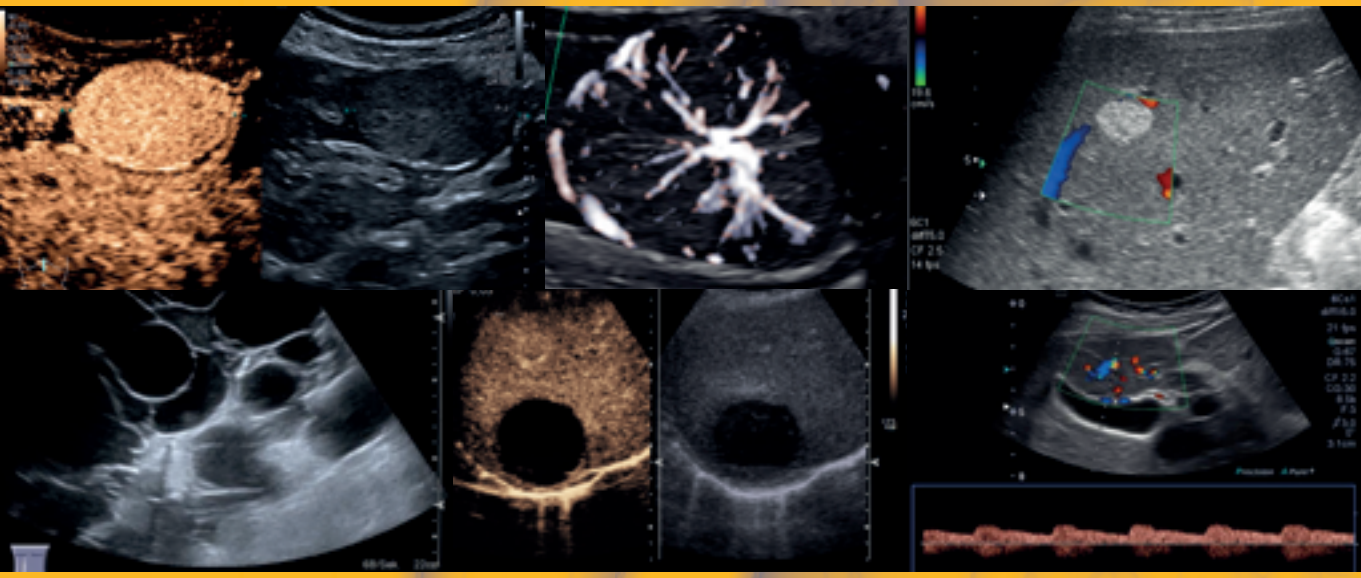

The information contained in this brochure is intended exclusively for physicians and pharmacists. The contents reflect current developments in medical science. For information on indications and dosage schemes of the drugs please refer to the current SPCs (summary of product characteristics). Product presentations, compositions, indications and safety information as referenced herein may differ from those in your country. For further information, please contact Dr. Falk Pharma GmbH, Freiburg (Germany) or your local Falk partner.

Address of the author

Prof. Dr. Deike Strobel
Department of Internal Medicine 1
University Hospital Erlangen
Ulmenweg 18
91054 Erlangen
Germany
deike.strobel@uk-erlangen.de

Publisher

FALK FOUNDATION e.V.

Leinenweberstr. 5
79108 Freiburg
Germany

www.falkfoundation.org

Image credits

Cover: Magic mine/Shutterstock
All figures, unless otherwise specified: Deike Strobel

1st edition 2020

Ultrasound of the Liver

Benign Liver Lesions

Deike Strobel
University Hospital Erlangen (Germany)

Contents

Foreword

Focal liver lesions comprise a broad spectrum of different tumor entities. When using ultrasound to determine the malignancy of a focal liver lesion, it is crucial that practitioners be aware of the patient's clinical context and be familiar with typical morphological diagnostic criteria. The majority of focal liver lesions can be reliably characterized by B-mode or color Doppler ultrasound, while contrast-enhanced ultrasound (CEUS) is a powerful tool for lesions that are inconclusive in B-mode alone. This booklet provides an algorithm for diagnosing focal liver lesions by ultrasound in routine clinical practice together with tips for contrast-enhanced ultrasound that have been proven in routine practice. Common forms of benign liver lesions will be the focus of this booklet. Representative B-mode or color Doppler images of typical cystic and solid lesions together with crucial diagnostic criteria for contrast-enhanced ultrasound are intended to provide short and concise aids for daily practice.

I would like to thank the Falk Foundation e.V. for initiating a new version of "Ultrasonography of the Liver" (in memory of Prof. Ochs). This booklet on benign liver lesions is dedicated to the patients and colleagues who have taught me so much and have joined me on my path of clinical ultrasound.

Erlangen, August 2019
Deike Strobel

Experience is perception that has been understood
(Immanuel Kant)

1 Introduction and clinical context

Focal liver lesions are common findings that are often discovered incidentally due to the increasing use of imaging procedures (ultrasound, computed tomography [CT], or magnetic resonance imaging [MRI]). The incidence of such "incidentalomas" varies between 5% and 50% depending on the patient population [Karhunen 1986]. It is always crucial to differentiate benign lesions from malignant lesions and primary hepatic tumors from secondary tumors (such as hepatic metastases).

The most common benign focal liver lesions that are discovered incidentally include developmental cysts, cavernous hemangiomas, and focal fat deposits or focal fatty sparing. Hemangiomas and focal nodular hyperplasia (FNH) are much more common in women and are typically asymptomatic; however, they do occasionally take on a mass-like appearance, in which case they may also cause upper abdominal pain. Less common entities include hydatid cysts, which have a lower prevalence in more northern countries, while the least common benign liver lesions include hepatocellular adenoma, inflammatory pseudotumors, cystadenoma, angiomyolipoma, and hamartoma.

The most common malignant lesions of the liver are metastases (approx. 45%), followed by hepatocellular carcinoma (HCC; approx. 28%) and cholangiocarcinoma (CC; approx. 4%) [Kasper et al. 2005]. Metastases most commonly originate from primary tumors of the gastrointestinal tract, followed by the lung, breast, urogenital tract, and skin.

Due to their characteristic appearances, the common forms of benign focal liver lesions – such as developmental cysts, hemangiomas in a healthy liver, or focal fat depositions and focal fatty sparing – can usually be characterized reliably using conventional B-mode ultrasound imaging. The differential diagnosis for focal liver lesions that cannot be classified by B-mode imaging ranges from common to very rare tumor entities (Table 1).

Malignant liver lesions	***755***	***Benign liver lesions***	***573***
Metastases	383	Hemangioma	242
Hepatocellular carcinoma	279	Focal nodular hyperplasia	170
Cholangiocarcinoma	44	Focal fat	30
Lymphoma	7	Regenerative nodules	23
Leiomyosarcoma	3	Abscess	20
Hemangioendothelioma	2	Hepatocellular adenoma	19
Angiosarcoma	2	Hydatid cyst	7
Hemangioendothelial sarcoma	1	Scar tissue	6
Sarcoma	1	Necrosis	6
Liposarcoma	1	Degenerative liver parenchyma	4
Plasmacytoma	1	Inflammatory pseudotumor	4
Dysplastic nodule	1	Hematoma	3
Hilar cholangiocarcinoma	1	Hamartoma	2
Mast cell tumor	1	Angiomyolipoma	1
Malignant lesion, not otherwise specified	28	Lipoma	1
		Peliosis hepatis	1
		Nodular regenerative hyperplasia	1
		Siderosis	1
		Benign lesion, not otherwise specified	32
Total of malignant and benign lesions			***1328***

Table 1: Incidence of benign and malignant lesions in contrast-enhanced ultrasound (DEGUM multicenter study: Contrast-enhanced ultrasound for the characterization of solid liver lesions not classifiable by B-mode imaging [source: Strobel et al. 2009]).

The process of differentiating focal liver lesions starts with basic clinical information: gender, age, ethnicity, and laboratory findings, as well as the presence of cirrhosis or an extrahepatic malignancy can all narrow the differential diagnosis of liver lesions.

According to a recent retrospective analysis of 45,319 hospitalized patients over a period of 10 years, the prevalence of benign liver masses identified by ultrasound is 15.1% and increases with patient age [Kaltenbach et al. 2016]. The most frequently-observed forms of benign liver lesions were focal fatty sparing (6.3%), cysts (5.8%), and hemangiomas (3.3%), while FNH was more rare (0.2%) and lesions such as hepatocellular adenoma were extremely rare (0.04%). Hepatic cysts were detected more frequently in patients of advanced age (0.8% < 30 years old vs. 38.5% > 70 years old). Hemangiomas were detected somewhat less frequently among young patients (7% < 30 years old); while the prevalence was 20% for patients between 40 and 70 years old. FNH and hepatocellular adenoma were primarily observed among young women.

Patient medical background can aid the classification of lesions detected by ultrasound:

I. Incidental findings
Lesions that are discovered fortuitously in the otherwise healthy liver of an asymptomatic patient are almost always benign. The most common forms of benign liver lesions are cysts and hemangiomas, as well as FNH in women. While metastasis should be suspected in patients with known cancer, even tumor patients can exhibit cysts and hemangiomas just like the healthy population. As a result of demographic changes leading to an ever-aging population, second primary cancers are no longer a rarity.

II. Infection or trauma
Anechoic lesions in patients with prior infection or trauma and typical clinical symptoms should raise suspicion for abscesses, hematoma, or post-operative fluid collection.

III. Liver cirrhosis
The differential diagnosis of a solid lesion can be narrowed considerably if cirrhosis can be detected clinically or by ultrasound. In the multicenter study by the DEGUM (German Society for Ultrasound in Medicine) on contrast-enhanced ultrasound for the characterization of liver lesions that were inconclusive by B-mode imaging, HCC comprised 76.6% of the lesions detected in cirrhotic livers. HCC can be differentiated from regenerative nodules by the presence of arterial hypervascularity with subsequent slow and mild hypoenhancement during the late phase of contrast-enhanced ultrasound [Seitz et al. 2011; Strobel et al. 2009; Wildner et al. 2015]. Cholangiocarcinoma is rare in a cirrhotic liver, and metastases are even more rare. Hepatocellular adenoma is never present in a cirrhotic liver. Hemangioma-like lesions in a cirrhotic liver may represent hyperechoic HCC. Therefore, every solid lesion in a cirrhotic liver should be considered to be HCC until proven otherwise.

IV. In patients with no clinical or sonographic evidence of cirrhosis, the differential diagnosis of HCC should also be taken into consideration upon observation of a solid liver lesion in a steatotic liver in men > 60 years old. Contrast-enhanced ultrasound can be helpful in this situation in order to confirm the diagnosis of HCC.

2 Diagnostic algorithm for focal liver lesions

Determining the prognosis and treatment requires answering the following questions:

– Can the lesion be classified as benign or malignant?
– Are further examinations necessary (staging, biopsy for histology)?

The following algorithm may prove helpful in diagnosing focal liver lesions (Fig. 1):

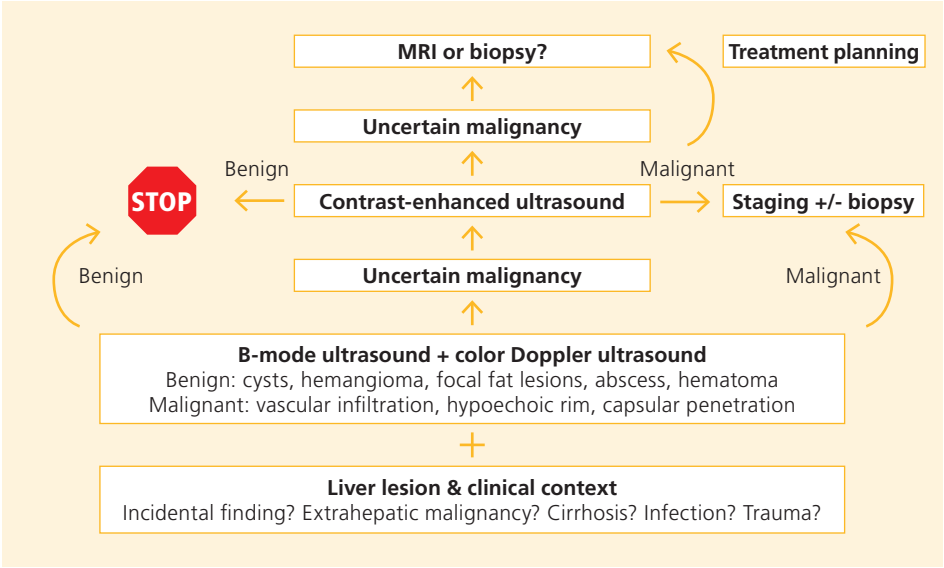

Figure 1: Diagnostic algorithm for focal liver lesions.

In patients with healthy liver parenchyma, common incidental findings such as developmental cysts or hemangiomas can be accurately diagnosed using B-mode ultrasound in combination with color Doppler. Focal fat depositions or focal fatty sparing can also be consistently identified by B-mode imaging alone in the hands of an experienced practitioner well-versed in ultrasound. If there is evidence that a lesion may be malignant, for example infiltration into the hepatic blood vessels (suggestive of HCC!), a hypoechoic rim (halo sign), or penetration of the capsule of the liver, histological confirmation using an ultrasound-guided biopsy is typically the most expedient route to definitively classify and grade the tumor entity.

Contrast-enhanced ultrasound (CEUS) is the primary method for determining the malignancy of lesions that remain inconclusive in color Doppler ultrasound. CEUS is efficient and has a high level of diagnostic reliability, enabling the correct classification of more than 90% of all lesions that cannot be classified by B-mode ultrasound [Strobel et al. 2008].

This approach saves time, is relatively inexpensive, and is also less stressful for patients. Moreover, contrast-enhanced ultrasound is also valued for its ability to visualize tumor-specific vascular patterns, thus saving patients the need for imaging methods that are expensive or expose them to radiation, such as computed tomography (CT) or magnetic resonance imaging (MRI), while also providing them a diagnosis more rapidly. If contrast-enhanced ultrasound is not possible or does not clarify the malignant nature of a lesion, liver MRI is the preferred non-invasive diagnostic method as it is superior to CT for the differential diagnosis of a focal liver lesion. Should a liver lesion remain inconclusive despite exhaustive imaging, ultrasound-guided needle biopsy is typically necessary. Further examinations will be required (staging, biopsy for histology) should the liver lesion prove to be malignant.

3 Contrast-enhanced ultrasound (CEUS)

Principles

Ultrasound contrast agents are comprised of microbubbles (< 10 µm) filled with gas that can diffuse through capillaries and through pulmonary circulation, which makes them a useful diagnostic tool for observing systemic circulation. These gas-filled microbubbles both reflect the ultrasound waves and also vibrate in response to excitement by the ultrasound waves, causing them to emit acoustic waves within a characteristic frequency spectrum. The ultrasound agents currently used in Germany are comprised of the inert gas sulfur hexafluoride (SF6) surrounded by an elastic phospholipid shell that reacts flexibly to the pressure generated in the acoustic field. Ultrasound devices require specific contrast software in order to perform contrast-enhanced ultrasound. This software allows the effects of the contrast agent to be selectively displayed while suppressing the majority of the tissue signal and movement artifacts. This technology is termed pulse inversion or phase inversion ultrasound and is currently available from all major manufacturers of ultrasound equipment. The energy used in the ultrasound signal is measured using the mechanical index (MI). Because excessive acoustic energy destroys the microbubbles containing contrast agent, low-MI techniques are currently practiced using low acoustic energy to allow for imaging in real-time.

Important: Contrast-specific software must be optimized for each individual device, even when using the latest generation of equipment. The user must become familiar with the use of the software provided with the ultrasound system. In order to avoid operator errors, it is crucial to receive proper instruction on the selected ultrasound system from the manufacturer's application specialists, especially for practitioners who have not previously used this technique.

The ultrasound contrast agents that are currently available do not extravasate from intact blood vessels, and are thus strictly intravascular contrast agents. Following intravenous administration, they are also highly specific for visualizing the smallest blood vessels and capillaries, allowing the vascular patterns of hepatic tumors and parenchymal perfusion to be visualized in real-time.

Administration of ultrasound contrast agents

Please refer to the appropriate Summary of Product Characteristics for information on the preparation of an ultrasound contrast agent.

Side effects, contraindications, and informing patient

In two retrospective studies with 23,000 and 30,222 applications of contrast agents, there were no deaths and the incidence of serious adverse events was 0.009% and 0.007%, respectively [Piscaglia et al. 2012; Tang et al. 2017].

Despite the fact that serious adverse events occur very rarely, it is still necessary to have emergency equipment and trained personnel on hand when administering ultrasound contrast media. Patients must be informed in writing about the indication and side effects prior to use.

Important: When administering ultrasound contrast agents, patients should be medically monitored, emergency equipment should be on hand, and personnel should be familiar with the procedures.

Additional links on the safety of contrast agents:

http://www.esur.org/esur-guidelines

http://www.efsumb.org/blog/archives/1156 – The WFUMB-EFSUMB Guidelines and Good Clinical Practice for Contrast Enhanced Ultrasound (CEUS) in the Liver: Update 2012

Examination procedure

The dual blood supply of the liver via the hepatic artery (25–30%) and the portal vein (70–75%) defines the vascular phases of the liver: the arterial phase, the portal venous phase, and the late phase. When using intravascular ultrasound contrast agents, practitioners must be familiar with the timing of these vascular phases, which in turn depends on the patient's individual cardiac output (Table 2). The volumes and lengths of injection of contrast agent are approximately 20-fold less than for CT or MRI. This allows the phases of contrast enhancement to be examined in real-time at a much higher temporal resolution than is possible using CT or MRI.

Sequence of contrast enhancement phases in the liver		
	Time after i.v. bolus injection (seconds)	
Phase	**Start**	**End**
Arterial	10–20	25–35
Portal venous	30–45	120
Late	> 120	approx. 240–360

Table 2: Vascular phases of contrast-enhanced ultrasound (source: Claudon et al. 2013).

Hepatic tumors have tumor-specific vascular architecture. The neoangiogenesis which is typical in hypervascular tumors can be visualized particularly well during the arterial phase of contrast enhancement. The real-time visualization of tumor-specific vascularity is especially important during two phases of hepatic perfusion when determining malignancy:

I. Early arterial/arterial phase of enhancement
(0 to approx. 30 seconds after i.v. bolus injection)

II. Late phase of contrast enhancement
(2 and 4 minutes after i.v. bolus injection)

Important: Use B-mode to determine the optimal position for imaging the liver lesion prior to performing contrast-enhanced ultrasound. Switching the patient to a left lateral decubitus position or using an intercostal transducer position may greatly improve the acoustic path, especially for lesions in posterior or subphrenic locations.

Early arterial/arterial phase of enhancement

In order to visualize the typical vascular patterns of tumors during the early arterial/arterial phase, images must be recorded continuously from immediately after the start of the bolus injection until contrast enhancement is detected in the tumor (between 10–30 seconds depending on hemodynamic factors). The region should ideally be scanned continuously in order to record the arterial vascular patterns of the tumor, as the first few seconds of contrast enhancement provide crucial information about tumor vascularity. The arterial enhancement phase should preferably be captured in the form of a video clip or a rapid sequence of images.

Important: Good communication with the nursing staff and the patient (briefly holding his or her breath, practice together with the patient before the injection if needed) is necessary to ensure optimal recording of contrast enhancement.

Criteria for determining malignancy during the early arterial/arterial phase of enhancement

The key question when using contrast enhancement is whether a typical tumor-like vascular pattern can be detected (Figs. 2–6):

– Central vascularity with radial vascular architecture is typical of FNH.

– Irregular blood vessels in the tumor with no identifiable pattern are typical of hypervascular metastases or HCC.

– Lesions which are primarily hypervascular with peripheral contrast enhancement are typical of hypovascular metastases.

– Hemangiomas exhibit no contrast enhancement during the initial arterial phase of enhancement, and then gradually display a thin ring of peripheral (nodule-like) contrast enhancement.

Portal venous phase and late phase

After the arterial phase, it is recommended that the liver lesion not be scanned for 2 minutes (freeze mode, leave transducer at the same position to prevent loss of the lesion, allow the patient to continue breathing calmly), and to wait until the late phase before resuming scanning. The early portal venous phase (45–90 seconds after bolus injection) provides little information that is useful for determining the malignancy of a focal liver lesion, as it is too early for metastases with arterial hypervascularity to exhibit hypoenhancement. Avoid excessive scanning when visualizing hemangiomas, as this may destroy the contrast enhancement in the capillaries – **Note:** this may cause pseudo-wash-out and lead to misinterpretation of the hypoenhancement as a malignant lesion.

Important: Continuous scanning after the arterial phase is counterproductive. Regular intermittent scanning (1–2 scans every 30 seconds over a period of 3–5 minutes) also harbors the risk of prematurely destroying the microbubbles.

Criteria for determining malignancy in the late phase (2 and 4 minutes after i.v. bolus injection)

It is essential to record and evaluate the late phase that begins after 2 minutes in order to determine malignancy. Typically, 1 (or max. 2) scans through the liver lesion are sufficient for recording contrast enhancement during the late phase. During this phase, the operator must focus on comparing the contrast enhancement within the liver mass with the enhancement of the surrounding liver tissue:

– Liver masses with contrast enhancement equivalent to or stronger than that of the liver tissue (isovascular, hypervascular) are considered to be benign.

– Liver masses that become enhanced by contrast agent but still appear hypoenhanced (hypoechoic) relative to the surrounding liver tissue during the late phase are considered to be malignant.

– Unique scenario of liver lesions in a cirrhotic liver: HCC exhibits a very long wash-out of contrast agent that usually starts after 3–4 minutes and is less prominent than wash-out from metastases. If there is no hypoenhancement after 4 minutes, or if there is insufficient contrast enhancement during the late phase, a second bolus of contrast agent should be administered in order to specifically assess the late phase after 4 and 6 minutes (without scanning before this time point).

Important: The ultrasound operator must be familiar with the anatomy and physiology of hepatic perfusion. Knowledge of tumor morphology is a prerequisite for characterizing focal liver lesions, as "you only see what you know". It may be helpful to consult pathology textbooks on the morphology of tumor vascularity.

Figure 2–6: Characteristic vascular and contrast enhancement findings.

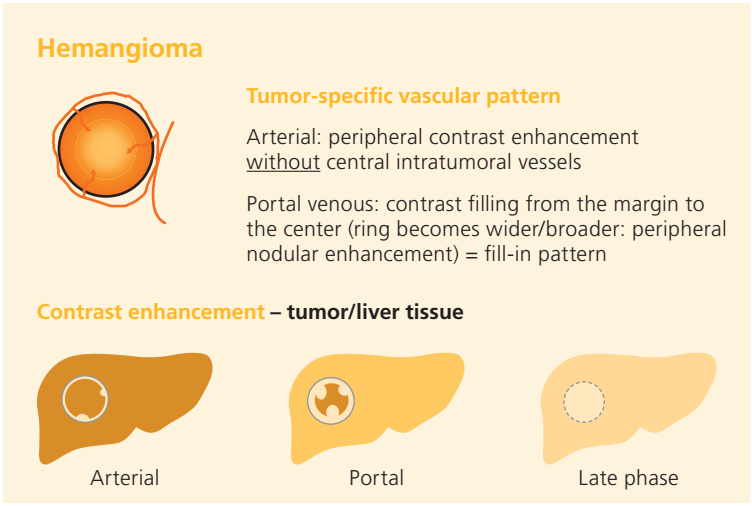

Figure 2: Hemangioma.

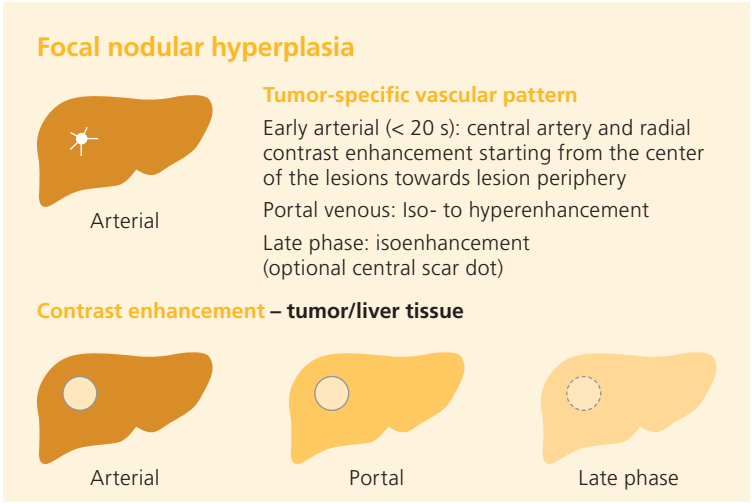

Figure 3: Focal nodular hyperplasia (FNH).

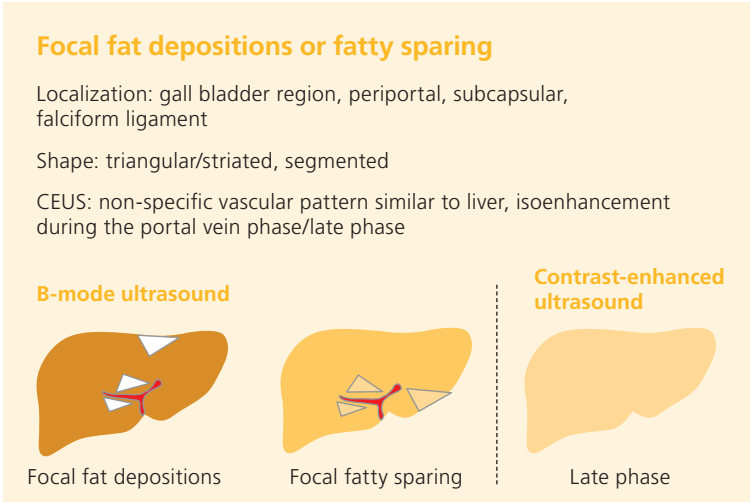

Figure 4: Focal fat depositions and fatty sparing.

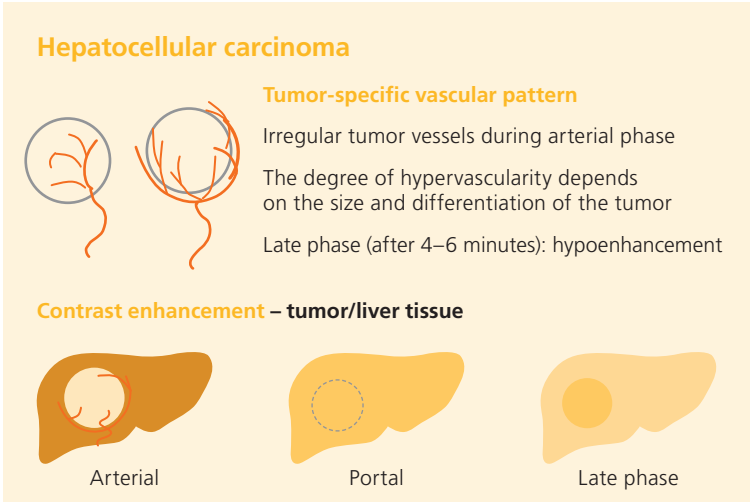

Figure 5: Hepatocellular carcinoma (HCC).

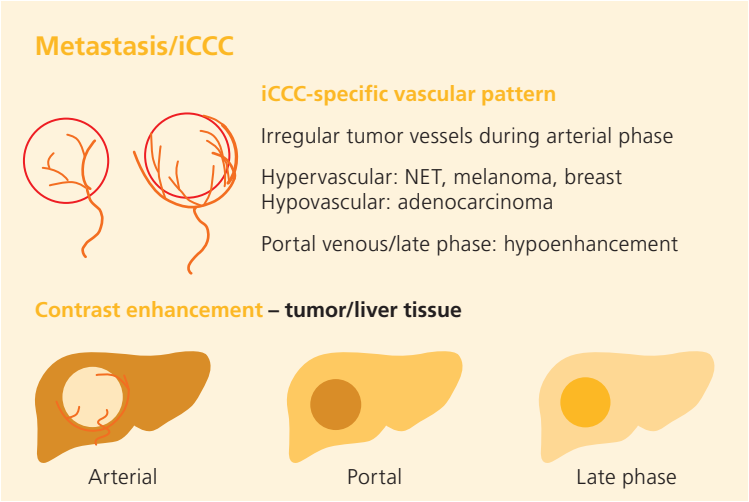

Figure 6: Metastasis/cholangiocarcinoma (CC).

Pitfalls with contrast-enhanced ultrasound

I. The differential diagnosis between partially thrombosed hemangioma versus hypovascular metastases is a particular challenge with small lesions. During the late phase, it is important to keep track of peripheral regions that also exhibited contrast enhancement in the arterial phase. Both of these entities exhibit regions of peripheral contrast enhancement during the arterial phase. However, very small intralesional blood vessels can be observed in hypovascular metastases (provided optimal ultrasound conditions) but not in hemangiomas. Therefore, it is also crucial to compare the changes in the contrast-enhanced regions of the tumor over time. Regions with contrast enhancement in the arterial phase and wash-out during the late phase are typically indicative of malignancy. Regions with contrast enhancement in the arterial phase and no change in enhancement during the late phase are typically indicative of partially thrombosed hemangioma (partial peripheral nodular enhancement).

II. It is important to record an additional time point during the late phase (4 minutes after injection of the contrast agent) if HCC is suspected or for focal liver lesions with robust contrast enhancement during the arterial phase. HCC in particular exhibits a late wash-out. The hypoenhancement of HCC lesions in cirrhotic livers typically cannot be detected until 3–4 minutes after injection.

III. Examination of multiple focal liver lesions: identical morphology in ultrasound (B-mode) suggests that the tumor entity is the same. Hypoenhanced lesions with suspected malignancy may become visible during the late phase of contrast-enhanced ultrasound. In cases of isoenhancement (homogeneous contrast enhancement across the entire liver without hypoenhanced lesions) in non-cirrhotic livers, any lesions present are benign. If different lesions in the same liver have different morphology on ultrasound, attempts should be made to visualize multiple lesions in one field of view (B-mode and contrast-enhanced ultrasound). Should this not be possible, a second bolus injection of contrast agent will be required for lesions with differing morphology.

Limitations of CEUS

All ultrasound techniques are hindered in patients with obesity or abdominal distension that limits the ability to evaluate their liver. For such patients, the use of liver MRI may be advisable for determining tumor malignant potential, as this technique does not expose the patient to radiation and is superior to CT for the characterization of tumors.

4 Cystic lesions

Simple hepatic cysts

Developmental cysts

Hepatic cysts are often incidental discoveries, and are observed in ultrasound more frequently with increasing age (0.8% < 30 years old vs. 38.5% > 70 years old) [Kaltenbach et al. 2016]. A typical hepatic cyst (Fig. 7) has no rim, posterior acoustic enhancement, and a completely anechoic interior. If these criteria are fulfilled and the cyst was an incidental discovery, no further examinations are necessary. Hepatic cysts may be solitary or multifocal. While the majority of cysts do not cause clinical symptoms, very large cysts may cause some symptoms such as a sensation of pressure due to organ displacement or localization near the capsule. Due to the great difference in impedance between hepatic cysts and normal liver structures, even cysts that are only a few millimeters in diameter can be detected. Benign developmental cysts can be easily differentiated from other hypoechoic masses or blood vessels based on typical sonographic criteria (Table 3).

– Anechoic contents
– Round shape
– Smooth, well-defined margins to surrounding tissue (no rim)
– Posterior acoustic enhancement
– Enhancement of the anterior and posterior margins
– Lateral shadowing ("edge artifact")
– No perfusion (color Doppler)

Table 3: Characteristics of simple hepatic cysts on ultrasound.

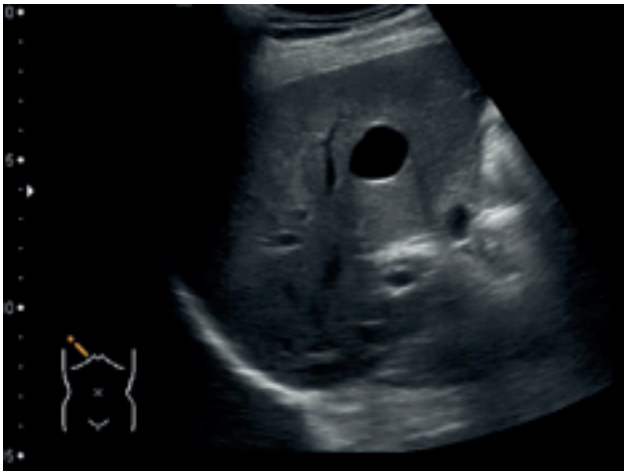

Figure 7: Typical cyst (round, anechoic contents, posterior acoustic enhancement, lateral cystic shadowing/edge artifact, enhancement of the anterior and posterior margins).

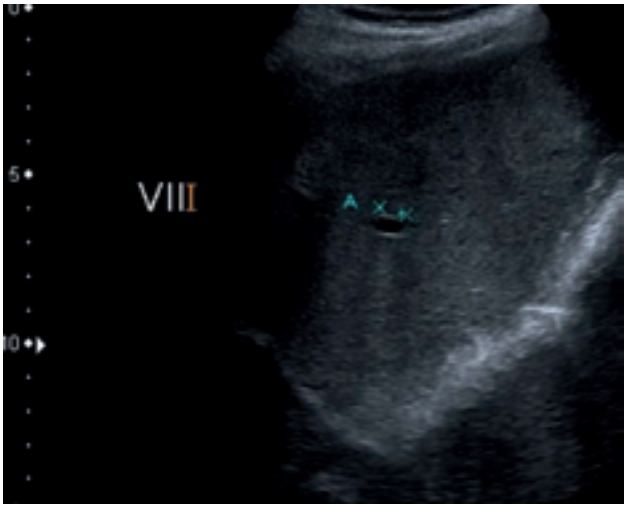

Figure 8: Small hepatic cyst (liver segment VII in zoom mode). Obvious enhancement of the anterior and posterior margins, posterior acoustic enhancement.

Polycystic liver disease

Polycystic liver disease denotes conditions characterized by multiple cysts throughout the liver resulting in marked hepatomegaly. The presentation often includes symptoms such as a sensation of pressure caused by stretching of the liver capsule and the displacement of adjacent organs (Fig. 9). These hepatic cysts can range in size from a few millimeters to several centimeters. The metabolic capacity of the liver remains durably intact even in the presence of multiple cysts. Patients with the autosomal dominant form of polycystic kidney disease will also have multiple non-communicating cysts located in the liver, as well as occasional lung, spleen, pancreatic, and ovarian cysts (Fig. 10).

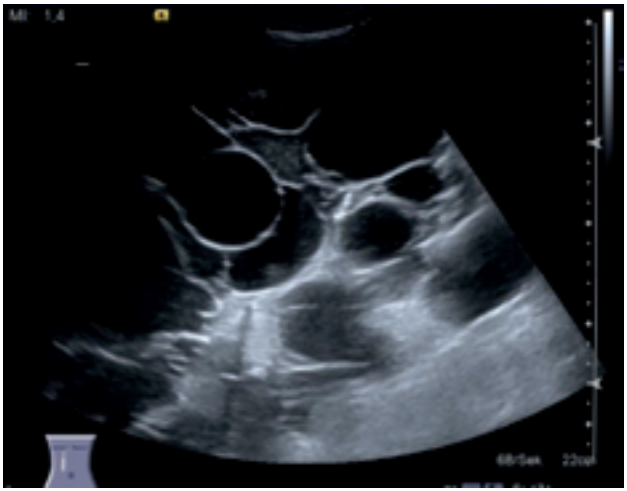

Figure 9: Polycystic liver disease. The liver extends into the mid-abdomen and is nearly completely filled with cysts. A small section of liver parenchyma is visible in the middle.

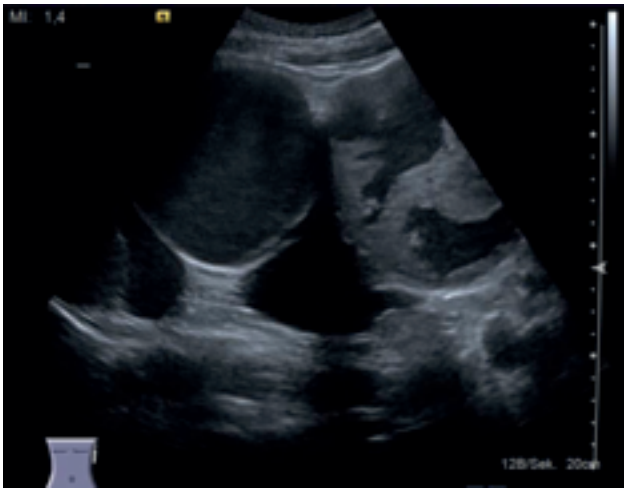

Figure 10: Polycystic liver with a polycystic kidney on left. The greatly enlarged liver is interspersed with numerous cysts and extends laterally to the far left, where it can no longer be delineated from the polycystic kidney. One cyst exhibits echogenic internal structures. A differential diagnosis of hemorrhagic cysts or solid cystic neoplasms must be considered for cysts with internal echogenicity. The solid components of the tumor are enhanced in contrast-enhanced ultrasound (see Fig. 41). Please refer to the Bosniak CEUS classification for the determination of malignancy of complex hepatic cysts [Rübenthaler et al. 2018].

5 Differential diagnosis of complex cystic lesions

Complex focal cystic lesions containing echogenic components or septations are markedly dissimilar to simple cysts. Hemorrhage, abscesses, cystic neoplasms, or parasitic cysts must all be considered as differential diagnoses depending on the clinical context. The combination of patient history and laboratory results together with characteristic ultrasound findings often provide the initial crucial hints for classifying complex cystic masses (Fig. 11). Diagnostic needle biopsy may also occasionally be useful. Contrast-enhanced ultrasound is not required if B-mode imaging and the clinical context already provide sufficient diagnostic information. However, contrast-enhanced ultrasound may indeed be helpful for identifying solid components of tumors in cystic neoplasms, as echogenic areas take up contrast agent during the arterial phase but display hypoenhancement during the portal venous phase indicative for malignancy [Corvino et al. 2017; Dong et al. 2017]. In patients with prior trauma or surgery, the administration of contrast agent can be used to detect active bleeding (extravasation of contrast).

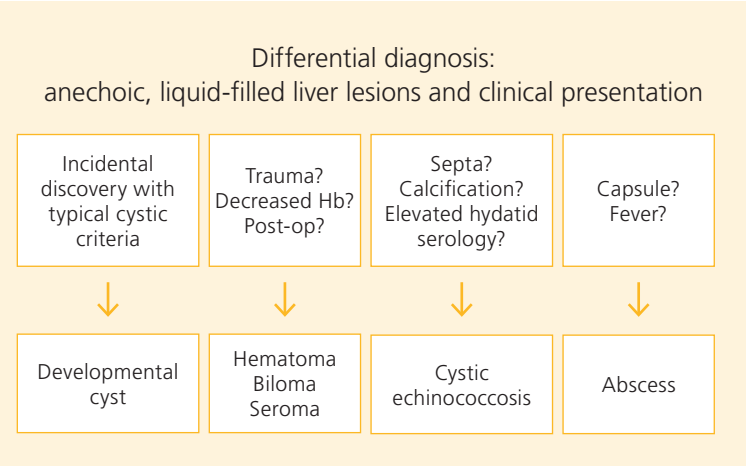

Figure 11

Septated developmental cysts

Developmental cysts can also occasionally exhibit delicate echogenic septa and multiple compartments. These cysts can be differentiated from cystic echinococcosis by the fact that the septa in developmental cysts tend to be delicate, and by the absence of the echogenic wall thickening that is typical of cystic echinococcosis. If there are any doubts, the patient's risk factors (such as contact with dogs) should be queried and parasite-specific antibody levels should be tested.

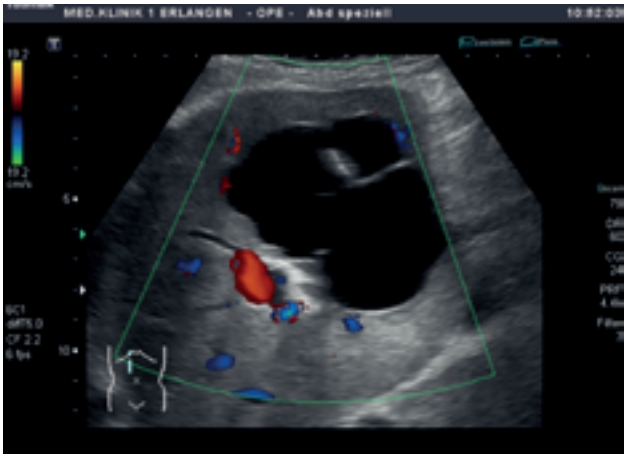

Figure 12: Developmental cyst with delicate septa (hydatid serology negative).

Hemorrhagic cysts

Delicate, homogeneous, and weakly echogenic cystic signals that float when the patient shifts position are suggestive of hemorrhage.

Case review: Echogenic cyst (Figs. 13a and b) before and after shifting position.

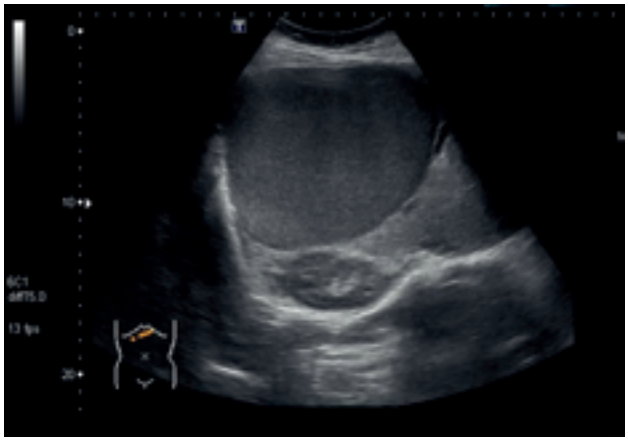

Figure 13a: Echogenic cyst in an asymptomatic patient.

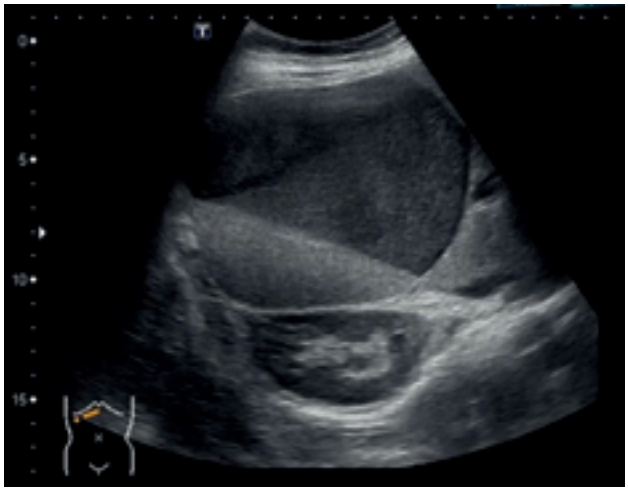

Figure 13b: Echogenic cyst. If some components of the cyst sediment after shifting position → differential diagnosis of a hemorrhagic cyst.

Hematoma

Sediment may be detectable in recent hematomas in patients with a suggestive clinical history (recent surgery or trauma). The patient's history and acute pain symptoms are crucial for diagnosing hematomas.

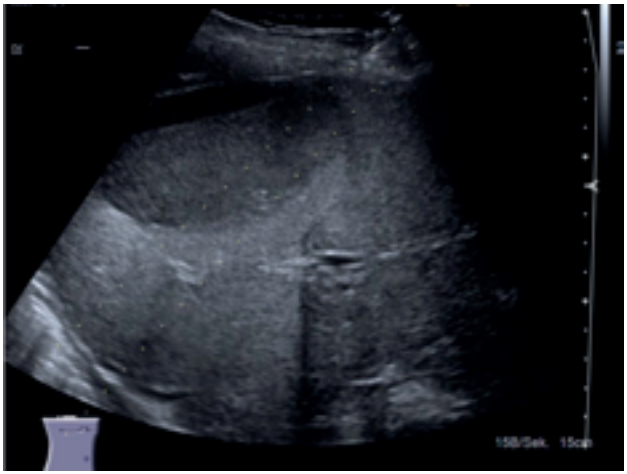

Figure 14: Recent hematoma (postoperative) in a symptomatic patient with local pain. The two dotted lines indicate the planned path for aspiration to drain the hematoma.

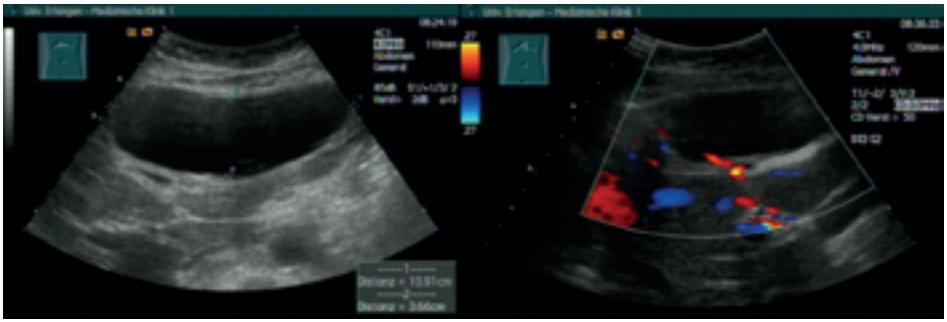

Figure 15: Recent hematoma (B-mode, color Doppler), clinical symptom of acute pain after lifting heavy loads.

Hematomas do not take up contrast agent in contrast-enhanced ultrasound. The detection of contrast enhancement in a fluid-filled, hypoechoic, or anechoic area may be indicative of ongoing bleeding (Figs. 16–18).

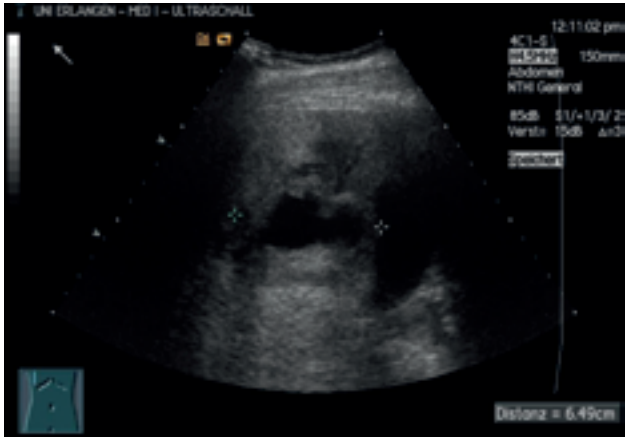

Figure 16: Hematoma following aspiration of a melanoma metastasis.

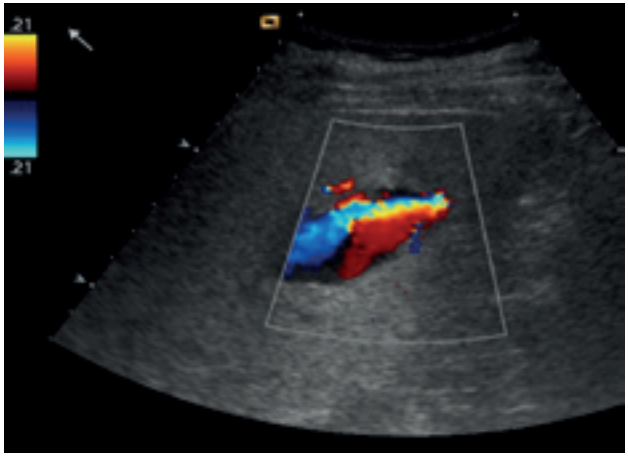

Figure 17: Active bleeding following aspiration (color Doppler: active bleeding).

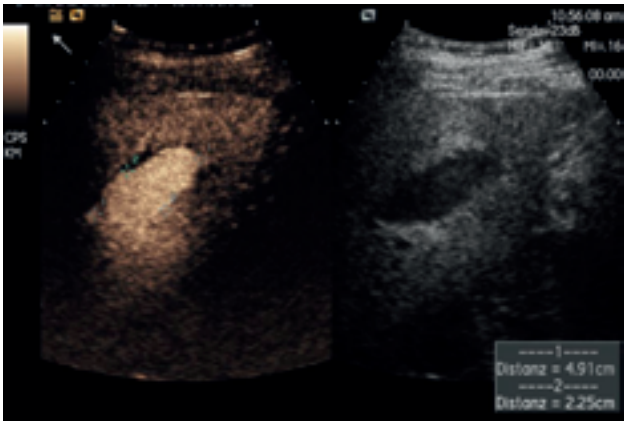

Figure 18: Active bleeding following aspiration (CEUS).

Abscesses

Pyogenic liver abscesses can be induced by streptococci, staphylococci, coliform bacteria, several different anaerobic species, and in rare cases by Yersinia species. The routes of infection for liver abscesses may be hematogenous (sepsis), hematogenous portal, ascending (cholangitis), or local spread (for example cholecystitis). The differential diagnosis is usually not difficult when the patient's clinical symptoms (fever, chills, right upper quadrant pain), laboratory findings (elevated C-reactive protein [CRP] levels), and history (for example surgery or travel abroad) are all taken into consideration.

Abscesses have a variable appearance in ultrasound that depends on both the age of the abscess and the extent of liquefactive necrosis (Table 4). The lesion often initially appears only as a hypoechoic lesion with ill-defined margins. As the untreated infection progresses, the surrounding tissue undergoes liquefactive necrosis (colliquation) and an echogenic capsule forms.

Appearance in ultrasound	Stage of abscess
Hypoechoic lesion with ill-defined margins	Focal inflammation without necrosis
Liquefaction → small anechoic areas	Early stage with focal accumulation of smaller abscesses which are still separated by areas of liver tissue
Larger anechoic/hypoechoic areas (late stage)	Contiguous abscess ± capsule

Table 4

An encapsulated liver abscess can be easily identified by ultrasound as an anechoic lesion with an echogenic capsule (Figs. 21, 22, and 25). However, differentiating between small, focal, inflammatory lesions during the early stages of liver abscess development and malignant focal liver lesions can prove difficult using either conventional B-mode ultrasound (hypoechoic, ill-defined margins) or contrast-enhanced ultrasound (contrast uptake during arterial phase, less enhancement during portal venous phase than surrounding liver tissue). Histology (pathology, microbiology) is usually required in order to confidently exclude malignancy.

Case review: Focal inflammation (Figs. 19 and 20):
Clinical symptoms: the male patient visited an emergency room due to deterioration of his general condition. He reported a history of prior gastrointestinal infection. CRP levels were slightly elevated. B-mode imaging revealed a hypoechoic lesion with ill-defined margins, while color ultrasound revealed hyperemia at the margins. The patient reported pain upon pressure by a targeted transducer placement. Malignancy was later excluded by biopsy.

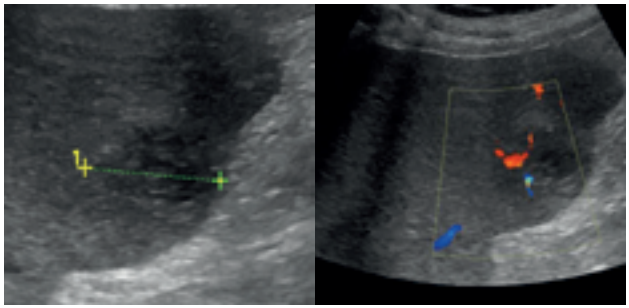

Figure 19: Focal inflammation (initial stage of abscess).

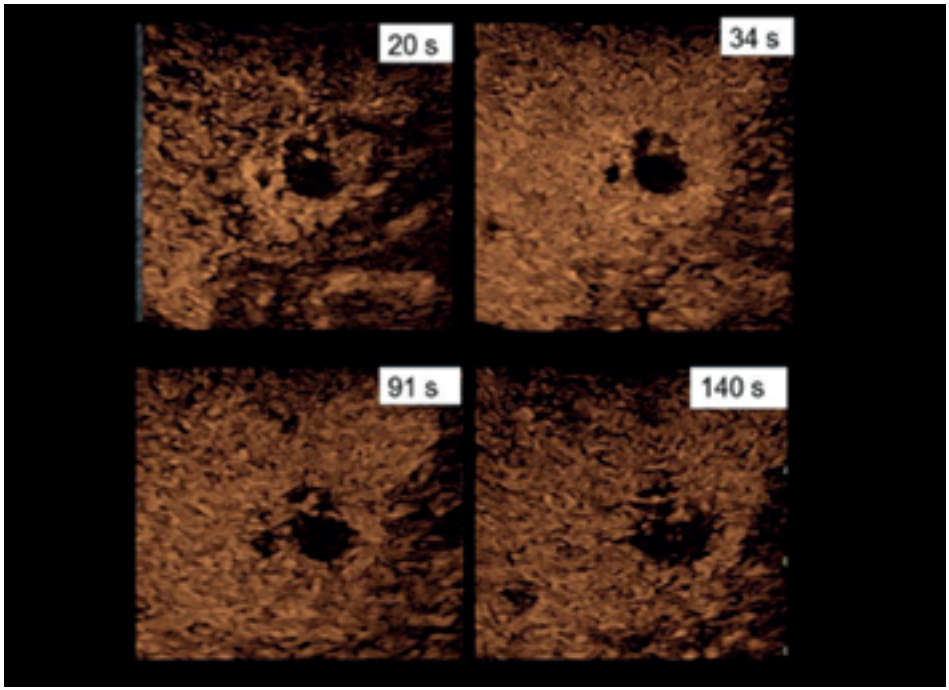

Figure 20: Focal inflammation (CEUS). Following administration of contrast agent, an avascular area becomes visible with marginal hyperemia initially detectable during the arterial phase (20 s p.i.).

It can be difficult to differentiate between small (< 2 cm) liver abscesses or inflammatory pseudotumors and malignant lesions (such as leukemic infiltration). A confirmatory biopsy is often required to exclude the possibility of a malignant lesion. CEUS may help clearly delineate avascular areas in small liver abscesses, which is useful for targeted ultrasound-guided needle biopsy.

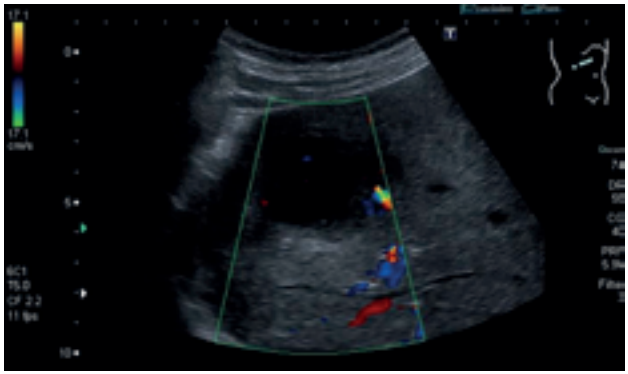

Figure 21: Abscess: liquefactive stage. Anechoic lesion with ill-defined margins, formation of a weakly hypoechoic capsule, and hyperemia in the surrounding liver tissue.

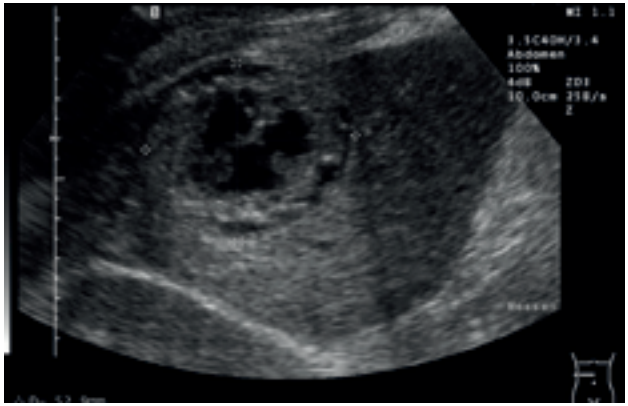

Figure 22: Older abscess with formation of an echogenic capsule. Depending on the clinical symptoms the differential diagnosis of a metastasis with central necrosis must be taken into account with this sonographic presentation (Fig. 24).

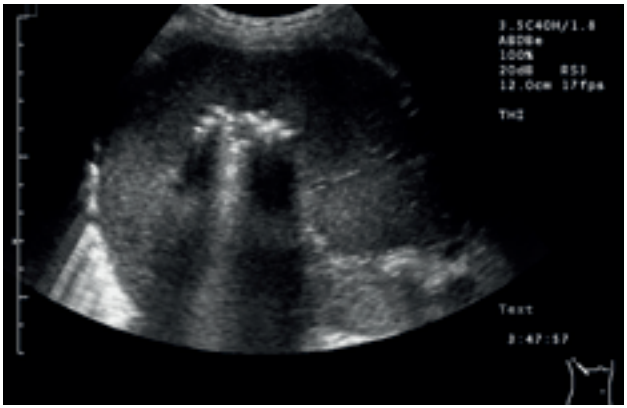

Figure 23: Liver abscess containing hyperechoic gas.

The presence of hyperechoic gas bubbles caused by bacteria is often overlooked or misinterpreted as calcification.

Liver abscesses exhibit no internal vascularity in color duplex ultrasound. Mature abscesses in the liquefactive stage do not take up contrast agent in contrast-enhanced ultrasound (CEUS) (Fig. 27), while the enhancement in the surrounding liver tissue displays hyperemia (Fig. 28). This reactive hyperemia in the adjacent liver tissue can sometimes even be detected by color Doppler (provided the settings on the color Doppler device are sensitive enough!).

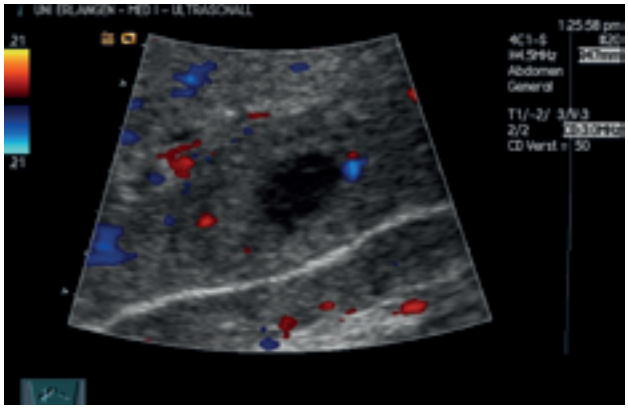

Figure 24: Metastasis with central necrosis.

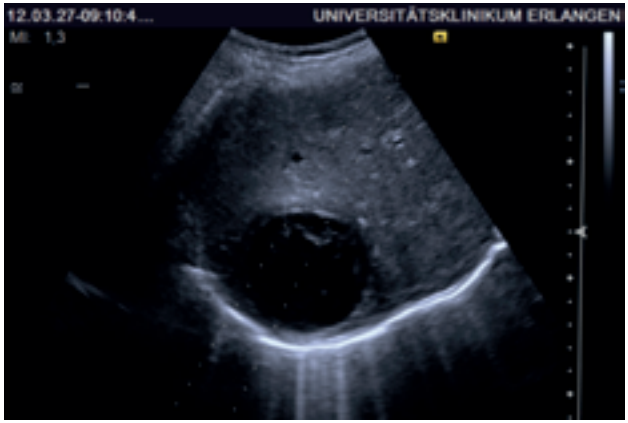

Figure 25: Liver abscess in liquefactive stage (B-mode). Internal echogenicity and thicker wall than cysts (see Fig. 7).

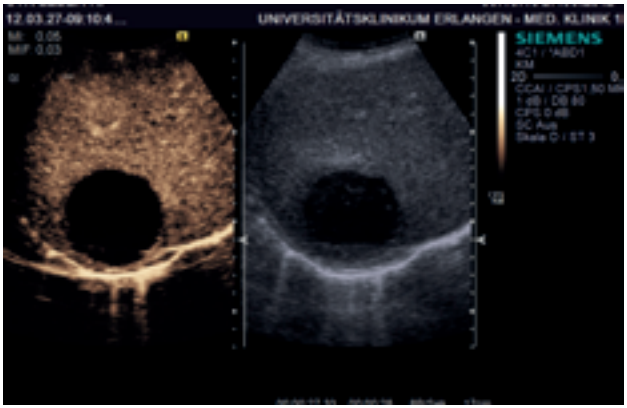

Figure 26: Liver abscess in liquefactive stage (CEUS).

The pathological stages of abscess formation (focal inflammation, liquefaction, coalescence into a solitary abscess, capsule formation) were characterized in a study on 115 liver abscesses. One typical appearance of a single abscess in CEUS is a delineated lesion with an avascular, fluid-filled center (with no contrast enhancement) surrounded by a hyperenhanced, hyperemic margin during the arterial phase. Transient hyperemia is visible in the surrounding liver tissue [Kunze et al. 2015]. Three stages of inflammatory liver lesions have been described using contrast-enhanced ultrasound: focal inflammation without necrosis, an early stage with focal accumulation of small pyogenic lesions separated by areas of liver tissue, and single abscess cavities surrounded by a capsule. Tiny, disseminated abscesses may also occasionally have no discernible pattern.

Case review: Hypoechoic focal infection, biloma → drainage (Figs. 27–29).

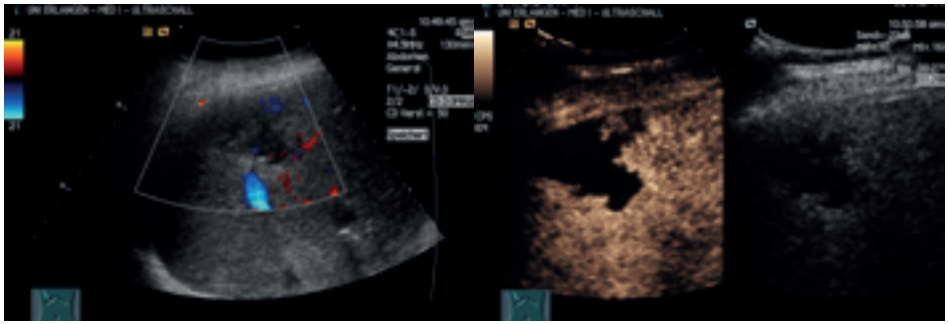

Figure 27: Initially hypoechoic liver lesion without anechoic fluid components in a patient with CC (Bismuth-Colette type 4). This area is avascular in contrast-enhanced ultrasound (no uptake of contrast), while the hyperemia in the surrounding liver tissue is noteworthy.

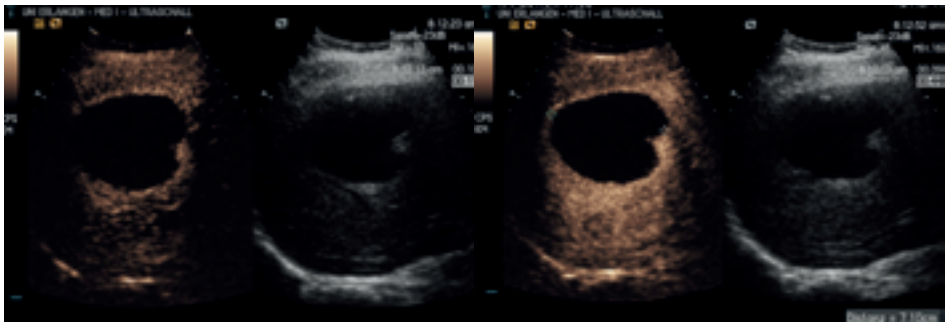

Figure 28: One week later, the lesion is filled with liquid (anechoic), has increased in size, and is now prominently demarcated from the liver tissue. It is avascular during the arterial and portal venous phases of contrast-enhanced ultrasound, with low-level hyperemia in the adjacent liver tissue.

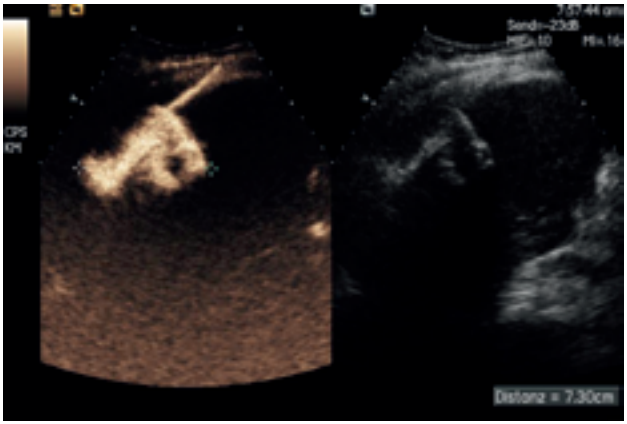

Figure 29: Drainage. Ultrasound-guided aspiration of the infected biloma was performed and the lesion was drained. The drainage was visualized by administration of 0.2 ml contrast agent plus 20 ml isotonic saline through the drainage.

Parasitic lesions

Cystic echinococcosis

Cystic echinococcosis (CE) can be identified very reliably using ultrasound depending on its stage. The most typical finding is a hyperechoic, thickened cyst wall containing multiple daughter cysts (WHO stage CE2). The morphology in ultrasound can be used to classify cysts into an active stage, a transitional stage, and an inactive stage. These cysts have typical morphologies in ultrasound, allowing experienced operators to reach a diagnosis rapidly in conjunction with serology testing. The World Health Organization (WHO) has proposed a classification scheme for cystic lesions (Fig. 30). Echinococcosis (hydatid disease) is a reportable disease in Germany, and must be reported anonymously to the Robert Koch Institute by laboratory physicians and clinicians alike. Laboratory diagnosis of the disease is performed by serology testing for parasite-specific antibodies in the patient's blood. It must be kept in mind that approximately 5% of cases of alveolar echinococcosis and 20–40% of cases of cystic echinococcosis (depending on organ involvement) may be seronegative.

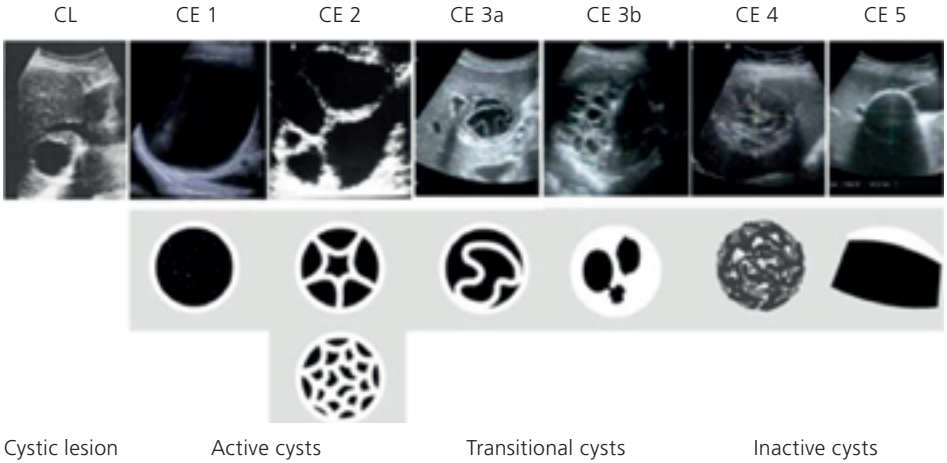

Figure 30: Overview of the WHO classification of cystic echinococcosis (CE) [Source: mod. from: Brunetti et al. 2010; usage in accordance with CC 4.0; https://creativecommons.org/licenses/by-nc-nd/4.0/]. This overview shows a typical cystic lesion (CL) on the left, followed by the stages of cystic echinococcosis. CE1 and CE2 are considered to be the active forms.

CE1 Oval-shaped cysts with thicker walls than for developmental cysts, but which are still often misinterpreted as hepatic cysts in this initial stage.

CE2 Cysts with daughter cysts.

CE3 Honeycomb structure. These cysts were no longer able to maintain their internal pressure. Rupturing of endocyst (water lily sign), floating membrane in primary cyst or onion skin-like intertwining of the two. Activity is transitional.

CE4 Solid tumor with potential calcification. Late, degenerative stage in which the solid components may possibly result from prior bacterial superinfection. The cyst takes on the appearance of a double membrane due to the close proximity of the cyst walls.

CE 5 Calcification (inactive form).

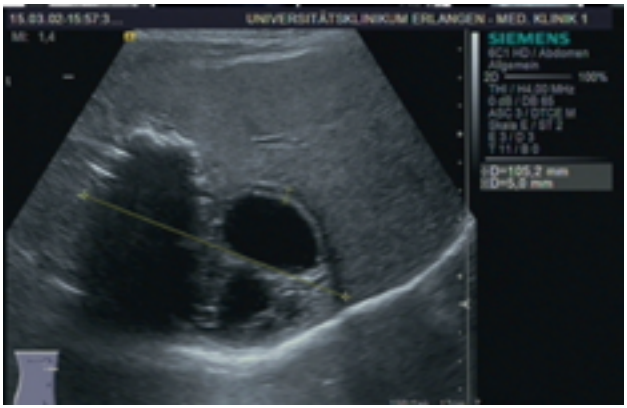

Figure 31: Echinococcosis (cystic form) with inactive cyst (calcification with posterior acoustic attenuation – WHO stage CE5) and active cyst (WHO stage CE2).

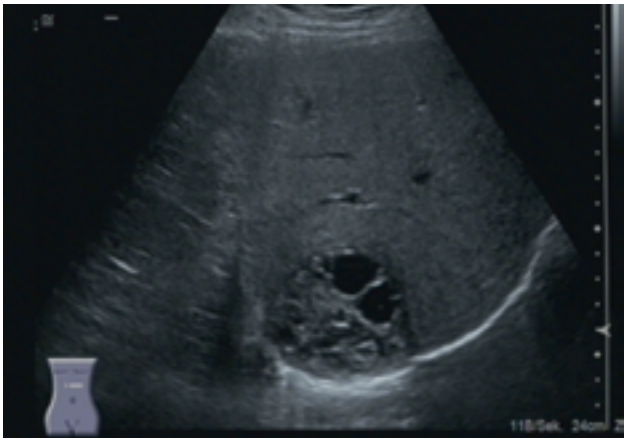

Figure 32: Cystic echinococcosis (transitional cyst CE3b). The fluid components of the cyst have clearly decreased, leaving the impression of a solid mass; minimal calcification visible.

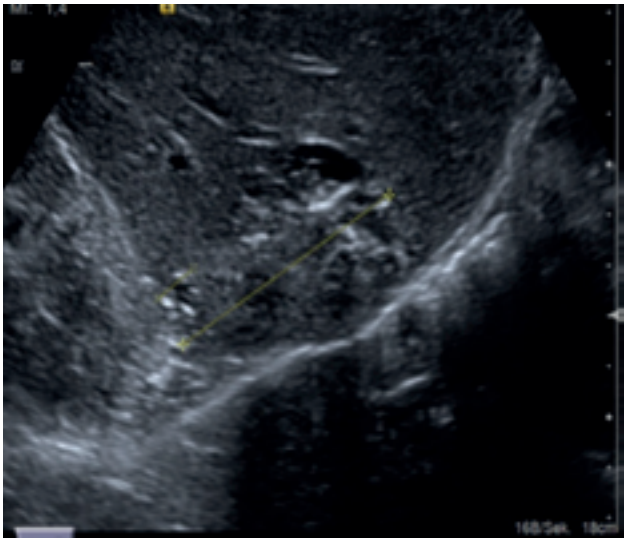

Figure 33: Cystic echinococcosis (CE4). Ultrasound image of a solid tumor with calcification (late degenerative stage).

Alveolar echinococcosis

The cystic form of echinococcosis (which comprises two-thirds of all cases) must be differentiated from **alveolar echinococcosis** (AE; infection with *Echinococcus multilocularis*), which tends to resemble a diffuse infiltrating tumor and is usually not anechoic. This disease is typically observed in the hilar region and is characterized by elevated levels of gamma-glutamyltransferase (GGT) and alkaline phosphatase (AP) in laboratory tests. Alveolar echinococcosis is a rare parasitic disease that is biologically characterized by infiltrative growth of a malignant neoplasm. If alveolar echinococcosis is diagnosed early enough, it can be resected following premedication with albendazole. The surgery – which should be as radical as possible – is accompanied by two years of subsequent albendazole therapy [McManus et al. 2003]. In contrast to the typical ultrasound appearance of cystic echinococcosis, the appearance of alveolar echinococcosis in cross-sectional imaging techniques is highly variable and is often the reason for misdiagnoses (CC, hemangioma, or metastasis). A retrospective study at the Ulm University Medical Center [Kratzer et al. 2015] analyzed ultrasound images from 185 patients with confirmed hepatic alveolar echinococcosis (over a period from 1999–2014).

The sonographic appearance of alveolar echinococcosis is highly variable (infiltrative liver lesions, potential malignancy). Hyperechoic, heterogeneous lesions with irregular contours and calcification are the most common form. The vascularity of these lesions cannot be visualized using color Doppler ultrasound.

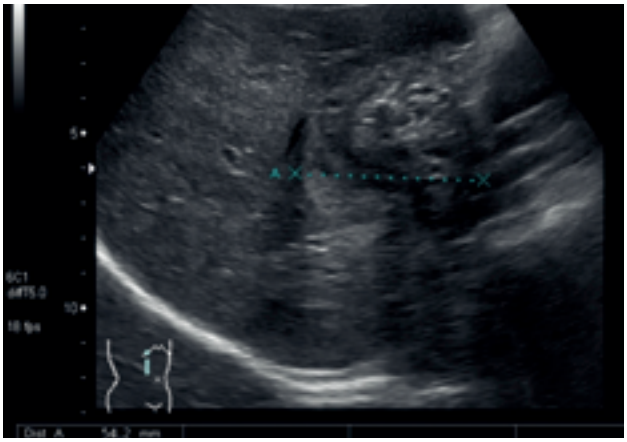

Figure 34: Alveolar echinococcosis (B-mode).

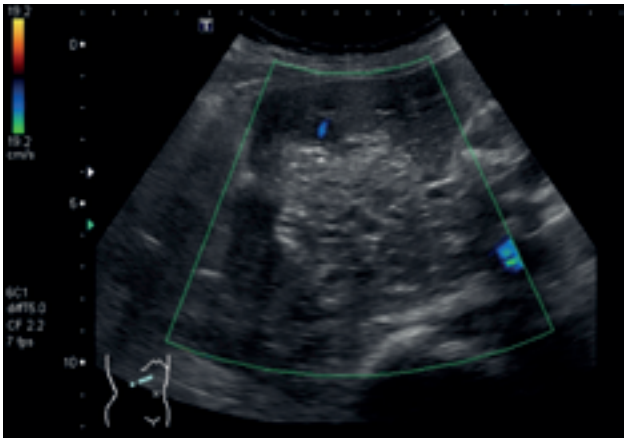

Figure 35: Alveolar echinococcosis (color Doppler).

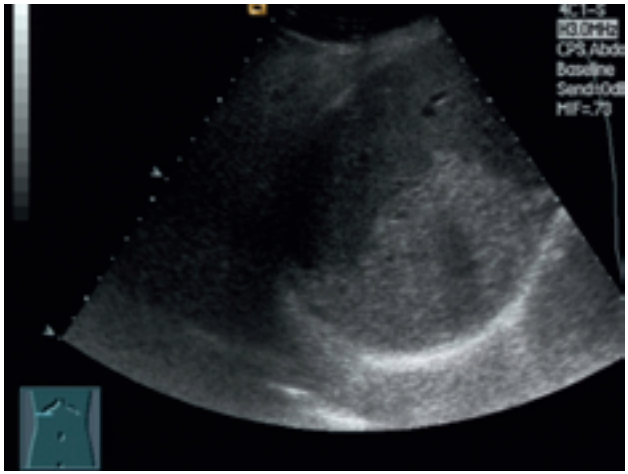

Figure 36: Alveolar echinococcosis (B-mode) with "hemangioma"-like appearance but irregular contours!

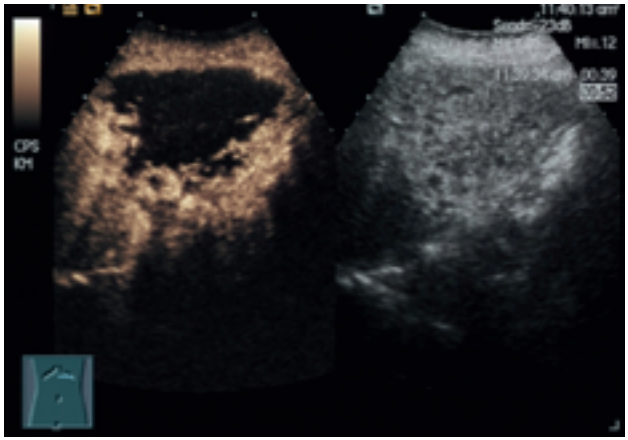

Figure 37: Alveolar echinococcosis (CEUS).

Alveolar echinococcosis appears mostly avascular in contrast-enhanced ultrasound (a crucial distinction from malignancies!), while vital cysts have thin rims with contrast enhancement.

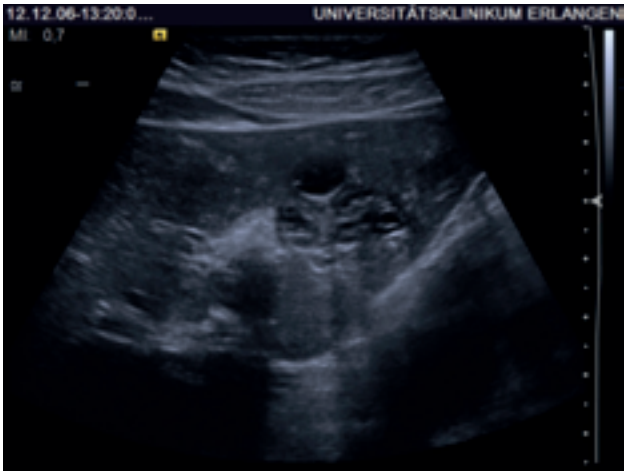

Figure 38a: Pseudocystic-like AE. The differential diagnosis between pseudocystic-like AE lesions or calcified lesions and cystic echinococcosis is difficult. This female patient was referred for ultrasound with a suspected diagnosis of Caroli syndrome based on MRI. In the end, alveolar echinococcosis was diagnosed (positive serology). The patient received premedication with albendazole followed by left hemihepatectomy (R0).

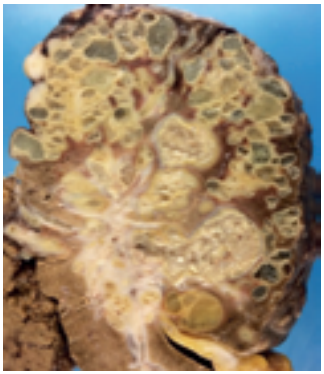

Figure 38b: Resected material. Infiltration of the left lobe of the liver by *Echinococcus multilocularis* (source: Institute of Pathology at the Sozialstiftung Bamberg, Germany, Prof. Dr. Gerhard Seitz)

Cystic neoplasms

Cysts with echogenic components require further examination. Metastases with central fluid collection (necrosis) are not unusual and are primarily observed in patients with rapid cancer progression. The echogenic components of cystic masses must be suspected of being malignant until proven otherwise. If the echogenic components appear vascular in contrast-enhanced ultrasound (contrast uptake), there is a differential diagnosis of a solid cystic neoplasm. If vascularity of the solid components is detected (CEUS), the lesion should be biopsied. Examples of cystic malignancies include cystadenocarcinoma of the liver (rare) or metastases with cystic components (e.g. ovarian cancer, gastrointestinal stromal tumor, and neuroendocrine tumors [NET]).

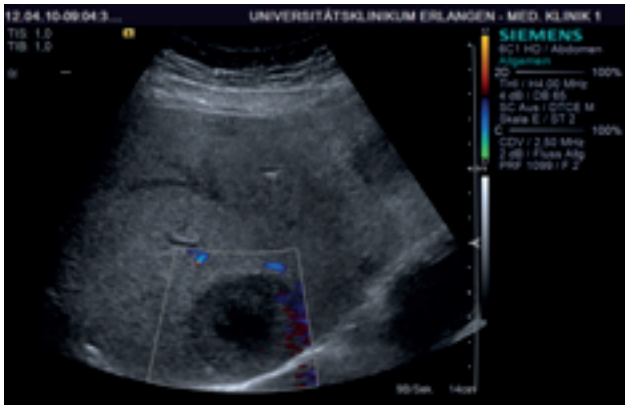

Figure 39: Metastasis (ovarian cancer) with central fluid collection.

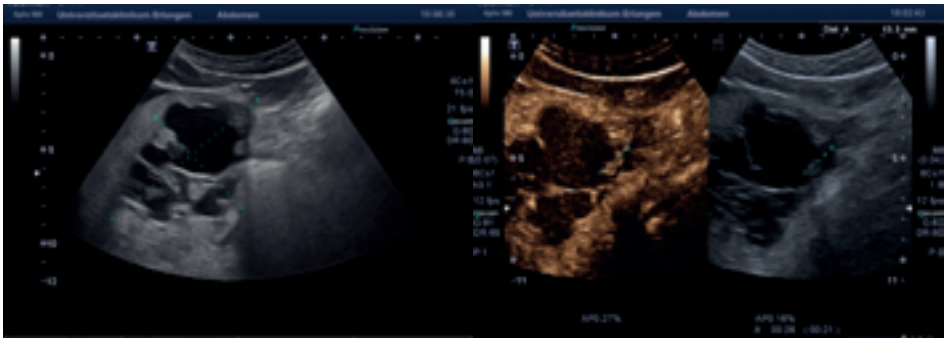

Figure 40: Cystadenocarcinoma of the liver (B-mode and CEUS). The echogenic components along the margin represent solid tumor mass. Ultrasound-guided needle biopsy of the solid components revealed cystadenocarcinoma of the liver. The tumor was already in an advanced stage with capsular penetration. CEUS: the echogenic components appear vascular in contrast-enhanced ultrasound (uptake of contrast, here after 21 s p.i.).

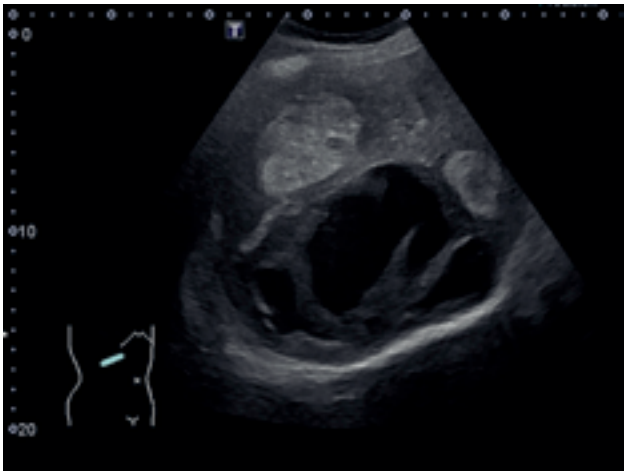

Figure 41: Metastases (solid and cystic) of a gastrointestinal stromal tumor.

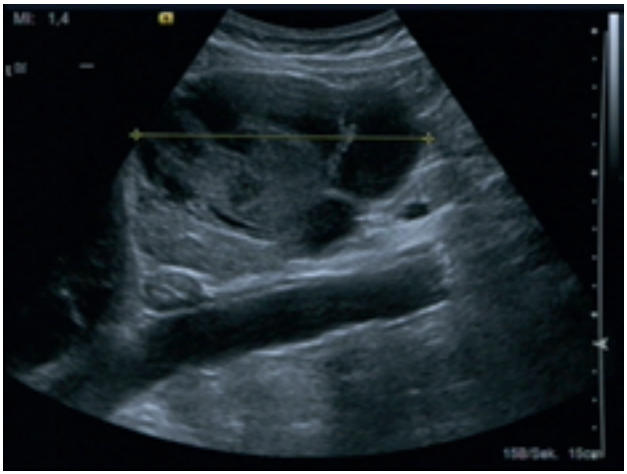

Figure 42: Solid cystic metastasis of a neuroendocrine tumor (rectum).

Pitfall: Caroli syndrome

Caroli syndrome is a rare, inherited cystic disorder of the bile ducts in conjunction with congenital hepatic fibrosis. The segmented, saccular dilation of the intrahepatic bile ducts (Figs. 43–46) may be misinterpreted as developmental cysts.

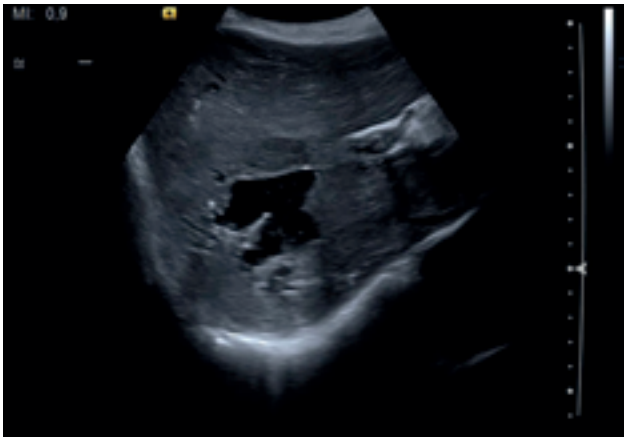

Figure 43: Saccular dilation of intrahepatic bile ducts.

Over the course of the disease, stones develop within the cystic dilations in the bile ducts (Figs. 44–46). Patients present clinically with relapsing cholangitis or biliary colic, as well as with signs of portal hypertension (splenomegaly, esophageal varices) at advanced stages of the disease.

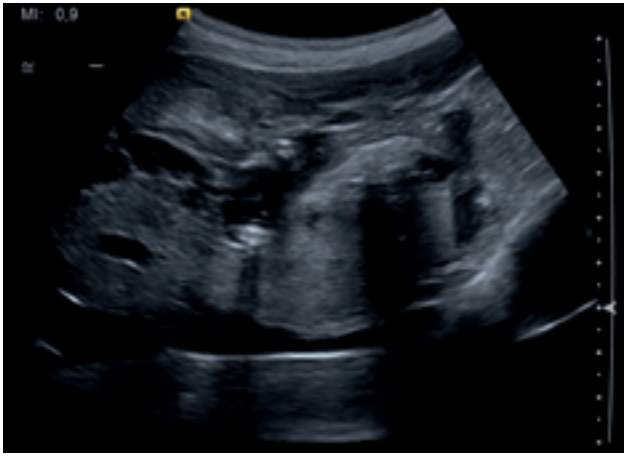

Figure 44: Dilated bile ducts, sludge in the left lobe of the liver.

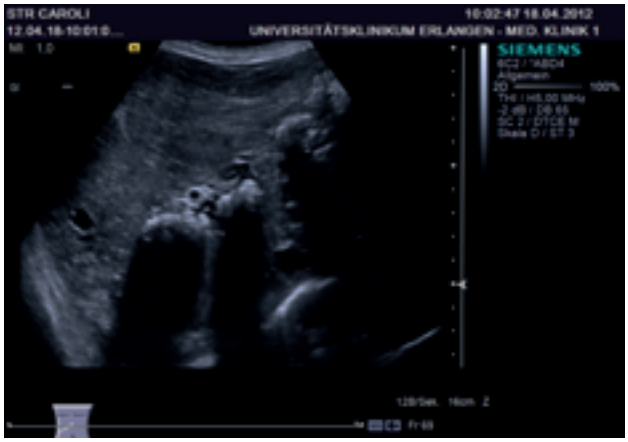

Figure 45: Hepatolithiasis.

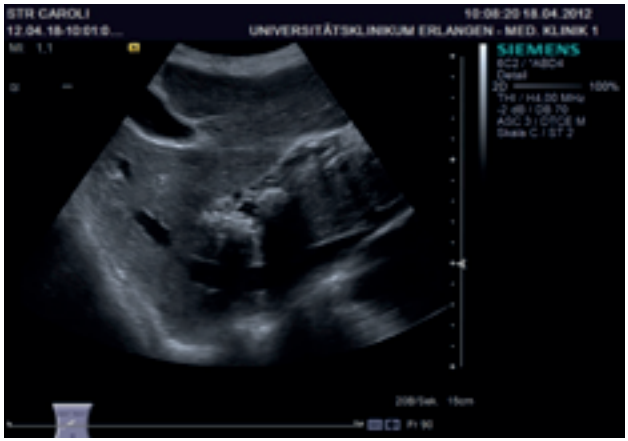

Figure 46: Hepatolithiasis.

Pitfall: Vascular malformation

Vascular malformation may closely resemble cysts in B-mode imaging. However, these two entities can be differentiated using color-coded blood flow in color Doppler mode.

Figure 47a and b: Vascular malformations. Cystic mass contacting a branch of the portal vein (B-mode), a vascular lesion is revealed in color Doppler (arterioportal shunt, **47a**). Additional example of an intrahepatic vascular shunt (2 cm) in zoom mode (**47b**) adjacent to a hepatic vein (portosystemic shunt). The blood vessels entering and leaving the malformation can be traced more easily by real-time examination.

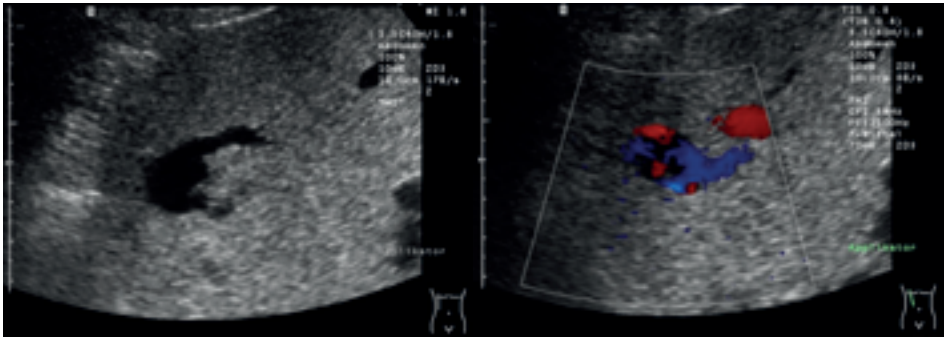

Figure 47a

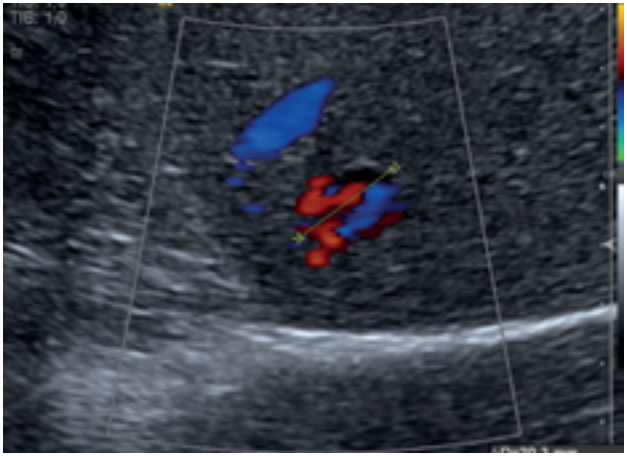

Figure 47b

6 Solid lesions

Hemangioma

Capillary hemangiomas represent the most common form of benign liver tumor diagnosed by ultrasound. The histological appearance of hemangioma is that of capillaries with slow blood flow and no mononuclear phagocyte system. As a hemangioma increases in size, it has a tendency toward thrombosis, fibrosis, cystic degeneration, or calcification.

Hemangioma with characteristic B-mode morphology

The typical morphology in ultrasound is that of a highly echogenic tumor with relatively smooth borders ("snowball"). It is often located close to a hepatic vein (Figs. 48 and 49).

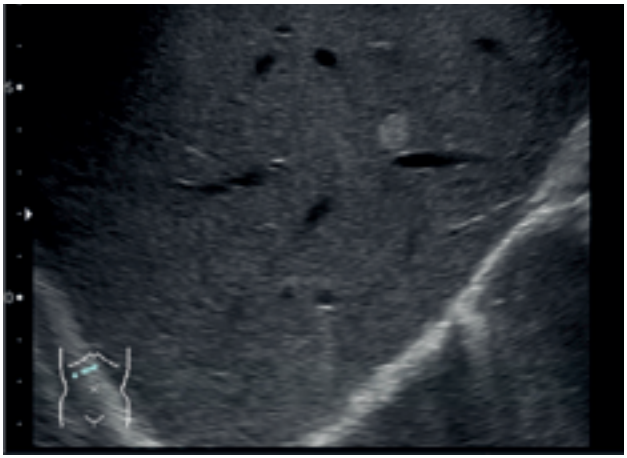

Figure 48: Typical hemangioma by B-mode. Hyperechoic hemangioma 1 cm in size with smooth margins, characteristic location near hepatic vein.

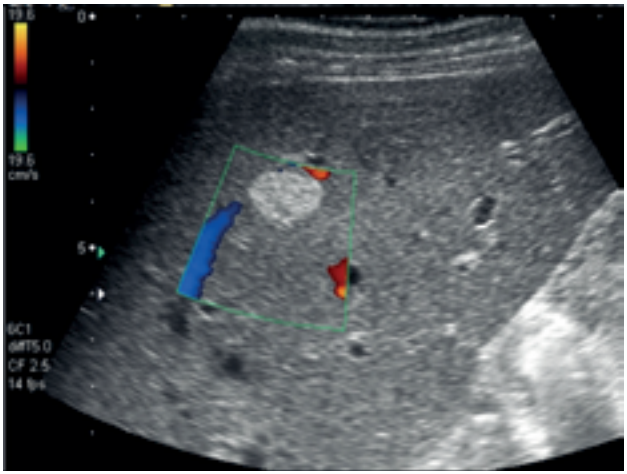

Figure 49: Typical hemangioma in color mode. Hyperechoic hemangioma 1.5 cm in size with smooth margins, near blood vessel. No color signal in hemangioma.

The characteristics listed above are typical for capillary hemangiomas which are rarely larger than 3 cm in size. Typical hemangiomas in a normal (non-steatotic, non-cirrhotic) liver in a patient with no clinical symptoms are considered to be sufficiently confirmed, and require at most a single follow-up after 3 months. Hemangiomas smaller than 3 cm in diameter display no signal in their center or at their periphery in color Doppler ultrasound (Figs. 49–51). The capillary flow in such very narrow capillaries is below the limit of detection of color or power Doppler ultrasound. If color signals are indeed detected in color mode, and especially if a pulsatile signal is received from the center of the lesion, a hypervascular tumor (for example a metastasis of neuroendocrine origin) should be suspected.

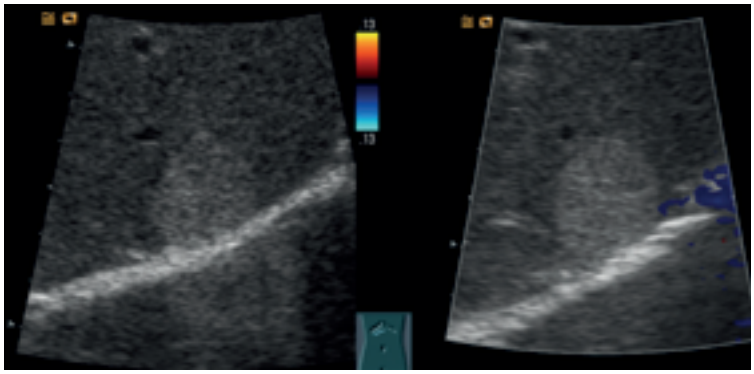

Figure 50: Hyperechoic, homogeneous hemangioma with smooth contours viewed in B-mode and color mode (zoom). No color signals can be detected from the hemangioma in color mode.

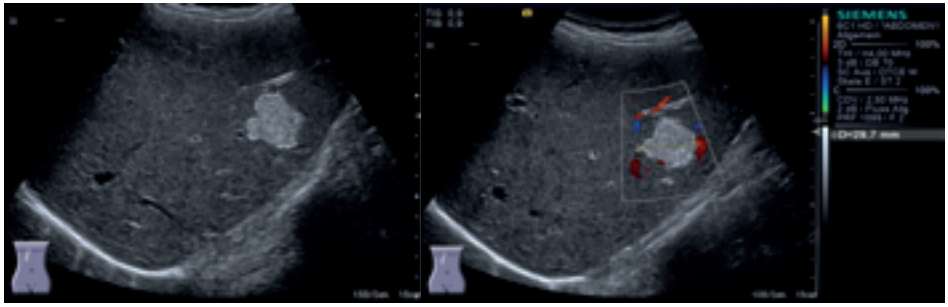

Figure 51: Hemangioma 3 cm large with irregular contours in B-mode (homogeneous, hyperechoic) and in color mode. No color signal in the hemangioma.

Hemangioma without characteristic B-mode morphology

Hemangiomas larger than 3 cm may be heterogeneous, and hypoechoic structures may represent thrombosis or fibrosis. If the identity of an uncharacteristic B-mode morphology is in doubt, contrast-enhanced ultrasound is the primary choice for further diagnosis, as it allows hemangiomas to be diagnosed very reliably based on peripheral nodular enhancement [Strobel et al. 2009].

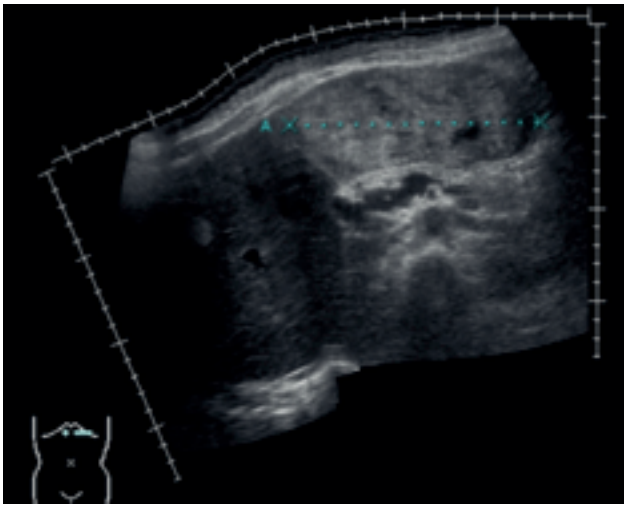

Figure 52: Asymptomatic female patient with a large hemangioma in the left lobe of the liver (panorama view). Measurements of the hemangioma in the left lobe: 13.4 x 8.5 cm (giant hemangioma). The patient had a second, smaller hemangioma in the right lobe (Fig. 53).

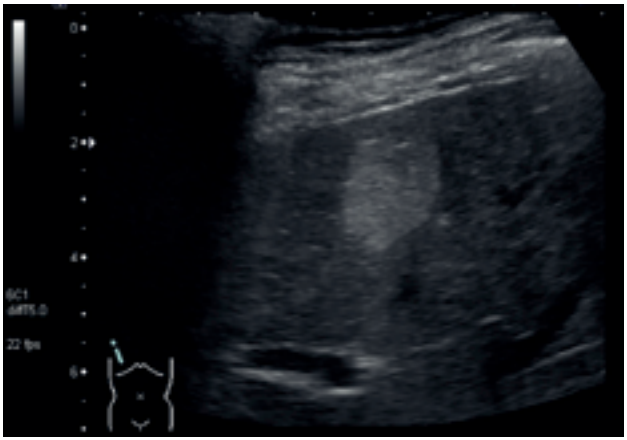

Figure 53: Hemangioma in the right lobe of the liver (intercostal transducer position).

Hemangioma in contrast-enhanced ultrasound

Following intravenous bolus injection of the ultrasound contrast agent, hemangiomas initially appear primarily avascular during the arterial phase, and small spots of enhancement are only visible in the periphery (termed peripheral globular enhancement). The hemangioma then fills slowly from its margins inward (peripheral nodular enhancement) owing to capillary blood flow, and in the late phase after 2–3 minutes it appears completely isoenhanced or hyperenhanced relative to the surrounding liver tissue. Peripheral nodular enhancement may be incomplete in very large hemangiomas.

Partially thrombosed hemangioma

Differentiation of partially thrombosed hemangiomas from hypovascular metastases: the nodular areas that are initially enriched in contrast agent after injection remain enhanced into the late phase!

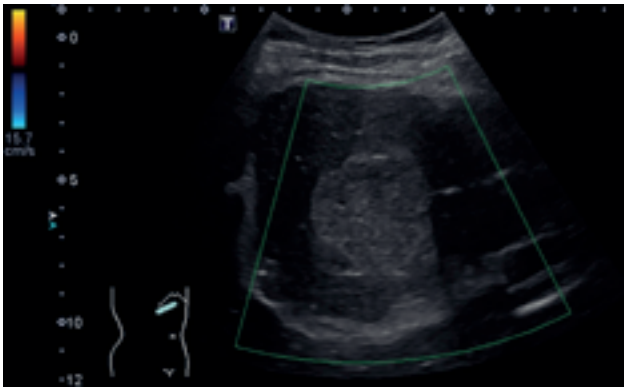

Figure 54: Hyperechoic, heterogeneous mass (6 cm) with ill-defined margins in B-mode → confirmation of the diagnosis of a partially thrombosed hemangioma by contrast-enhanced ultrasound owing to (incomplete) peripheral nodular enhancement (Figs. 55 and 56).

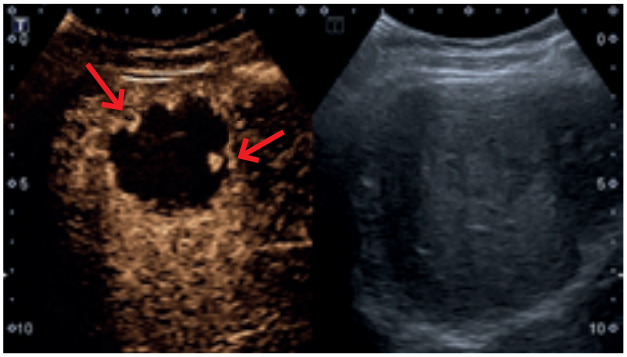

Figure 55: Contrast-enhanced ultrasound: the hemangioma appears primarily avascular after administration of contrast agent, although small nodular spots of enhancement are visible at the margin (arrows).

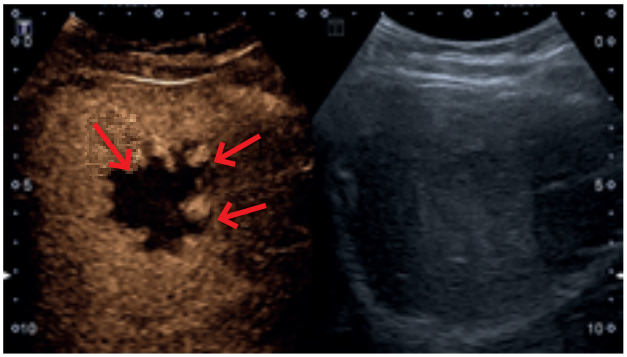

Figure 56: Partially thrombosed hemangioma (late phase of contrast-enhanced ultrasound 2–3 min p.i.): the hemangioma still appears to be mostly avascular, but the number and size of nodular spots of contrast enhancement (arrows) are increasing. An important criterion for differentiating these lesions from hypervascular metastases is the absence of enhancement wash-out from the nodules.

Hypoechoic hemangioma

In the steatotic liver, hemangiomas are hypoechoic and cannot be differentiated from other solid masses by B-mode imaging. The use of contrast-enhanced ultrasound is indicated in this situation, as the hemangioma can be accurately diagnosed by peripheral nodular enhancement (Figs. 57 and 58). In a nationwide, prospective study of contrast-enhanced ultrasound in Germany by DEGUM [Strobel et al. 2008, Strobel et al. 2009], 82.2% of hemangiomas whose identity was uncertain by B-mode imaging could be diagnosed using contrast-enhanced ultrasound.

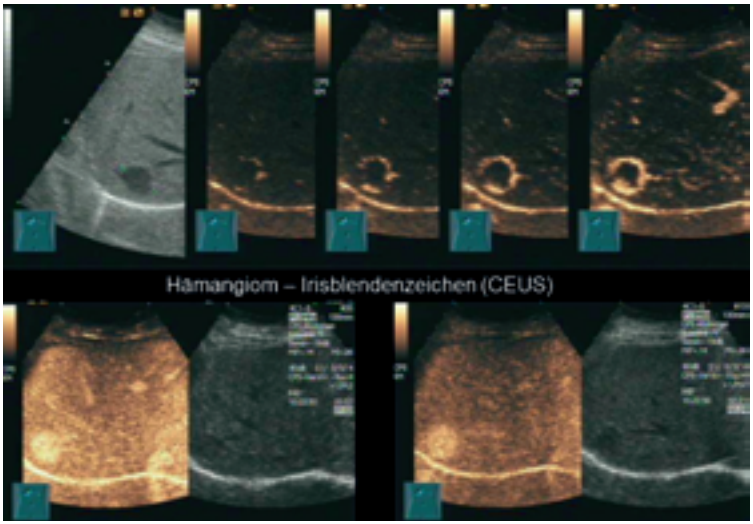

Figure 57: Hypoechoic hemangioma.
Upper row: B-mode image of a 2.5 cm hypoechoic mass on the left side in a steatotic liver. The subsequent sequence shows the contrast enhancement during the arterial phase (peripheral nodular enhancement).
Lower row: The lesion appears hyperenhanced relative to the surrounding liver tissue after 1 and 2.5 minutes (simultaneous contrast mode and B-mode).

Figure 58a and b: Hypoechoic hemangioma with hyperechoic rim.

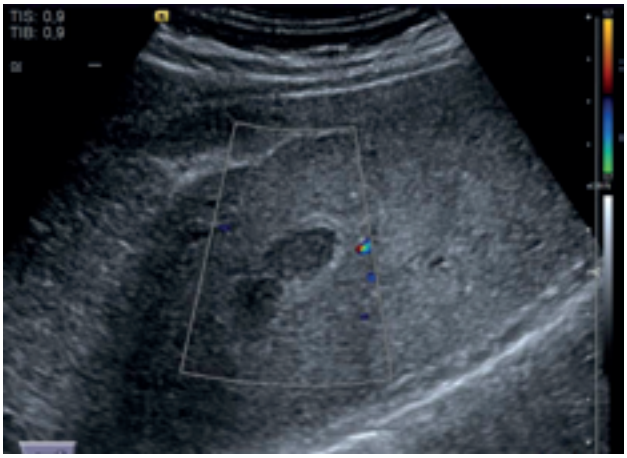

Figure 58a: B-mode image of hemangioma with oval shape, hypoechoic with hyperechoic rim. The capillary flow is below the limit of detection of color or power Doppler ultrasound.

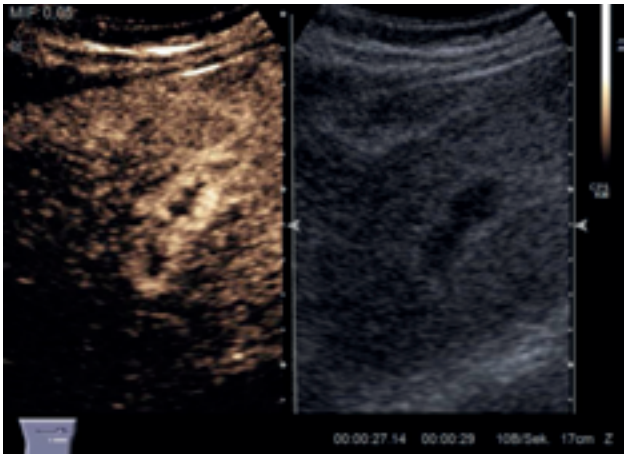

Figure 58b: Contrast-enhanced ultrasound: contrast enhancement and peripheral nodular enhancement (27 s p.i.). The dynamic process of complete peripheral nodular enhancement can be seen in the video sequences.

Case reviews

Case reviews 1 and 2: Both patients were referred with suspected diagnoses of hemangioma.

Case review 1

Asymptomatic male patient – incidental finding. The lesion was primarily hyperechoic, heterogeneous, and irregular by B-mode, and avascular in color mode (Figs. 59 and 60).

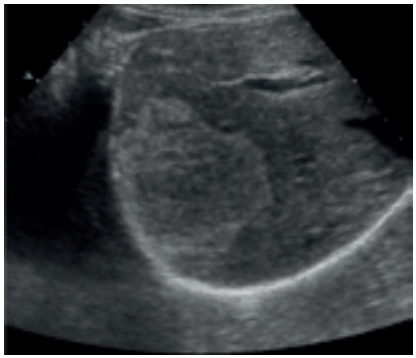

Figure 59

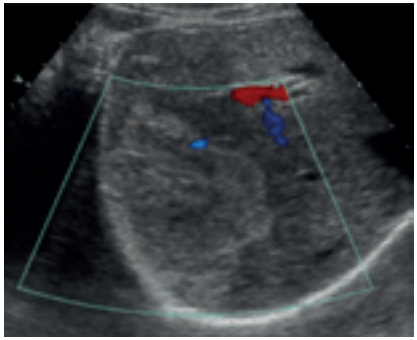

Figure 60

Contrast-enhanced ultrasound reveals peripheral contrast enhancement, the lesion is still mostly avascular. After 2 and 3 minutes, contrast-enhanced ultrasound reveals nearly complete peripheral nodular enhancement (Figs. 61–63).

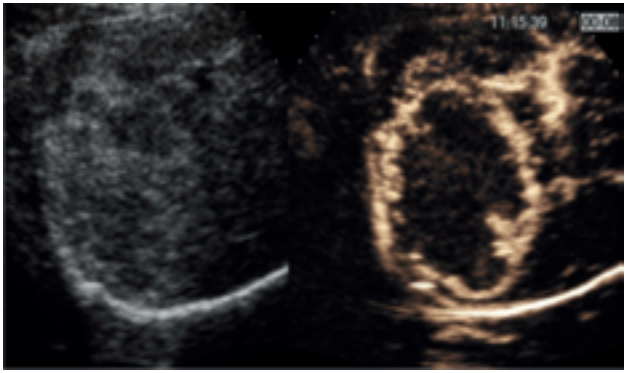

Figure 61

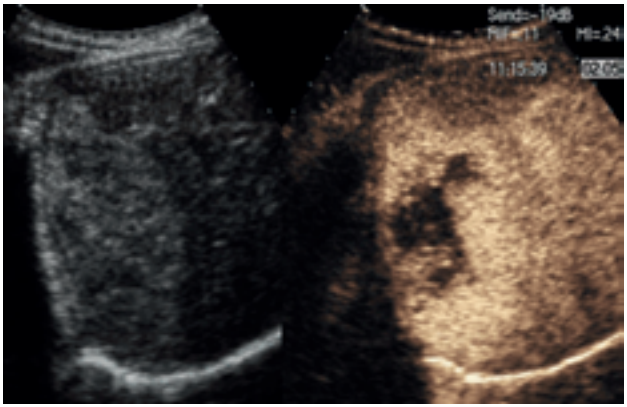

Figure 62

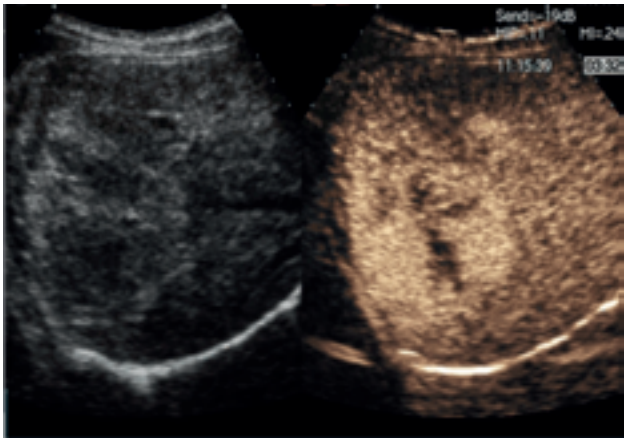

Figure 63

Diagnosis: partially thrombosed hemangioma. Follow-up examinations to check the size of the lesion by ultrasound were arranged upon request by the patient.

Case review 2

History of known hemangioma for 16 years (multiple ultrasound, CT, and MRI), the slow growth in size was noteworthy and hence the 54-year-old male patient attended for a second opinion. B-mode imaging reveals a heterogeneous tumor with cystic regions (Fig. 64).

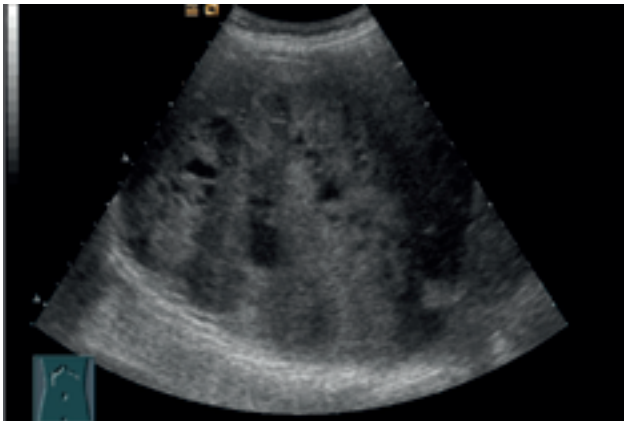

Figure 64

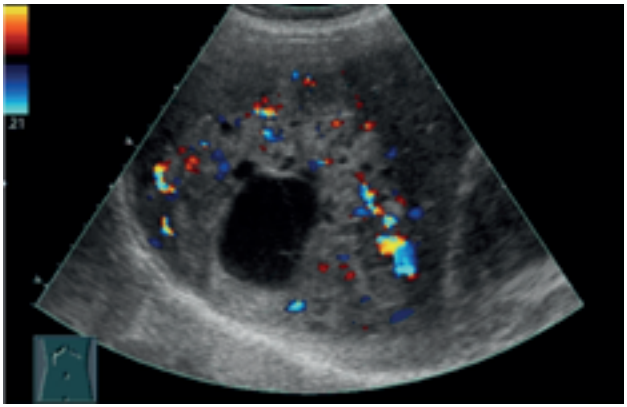

Figure 65

Color mode reveals small blood vessels in the solid region of the tumor that are atypical of hemangioma (Fig. 65).

Contrast-enhanced ultrasound (enhancement at 17 s and 21 s p.i.) shows a hyper-enhanced lesion during the arterial phase reminiscent of a hypervascular tumor, except that the cystic regions remain avascular. The tumor becomes enhanced much earlier than the rest of the liver, and small blood vessels can be seen in the surrounding liver tissue that drain the tumor (Figs. 66 and 67).

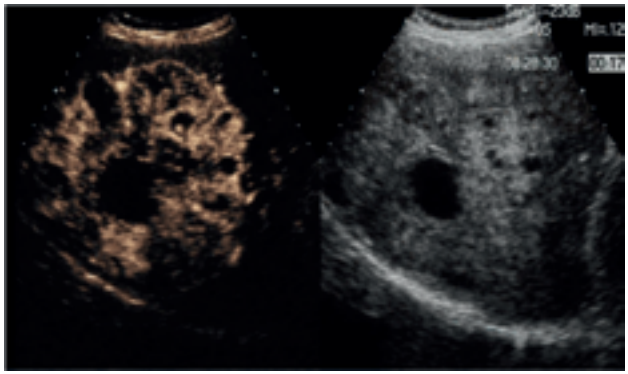

Figure 66

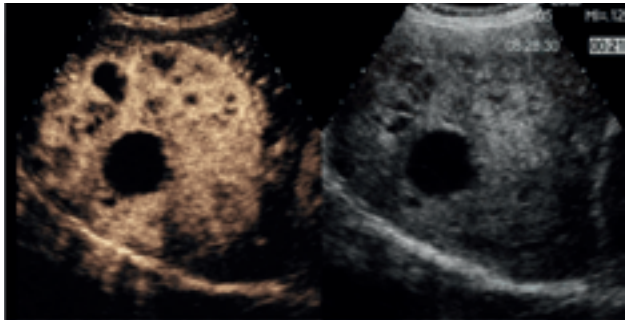

Figure 67

In the late phase of contrast-enhanced ultrasound (2.12 min and 2.47 min p.i.), the solid, vascular areas of the tumor are hypoenhanced relative to the surrounding liver tissue (wash-out, Figs. 68 and 69).

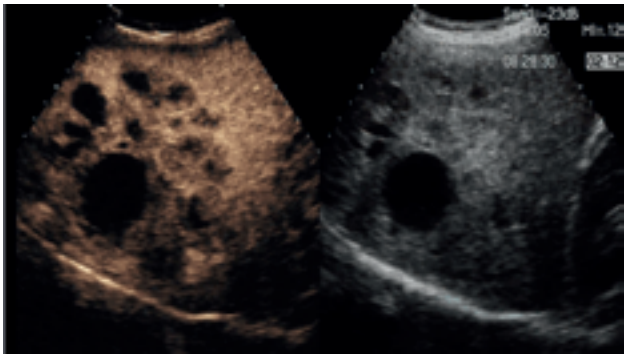

Figure 68

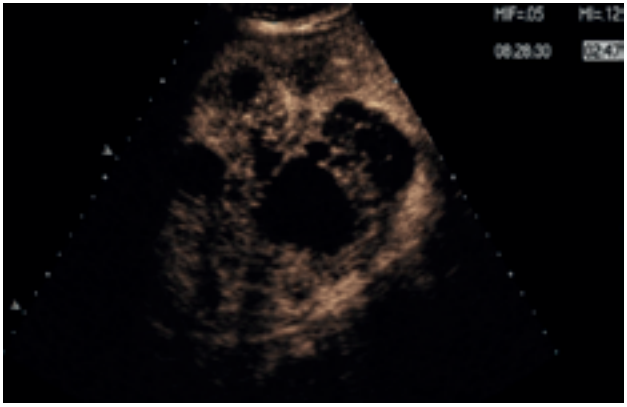

Figure 69

Diagnosis: The patient was clinically asymptomatic with no history of cancer or parenchymal liver disease, the remainder of the liver was unremarkable. Following contrast-enhanced ultrasound, which revealed a vascular pattern suggestive of a malignancy, a biopsy and eventually resection were performed. Histological diagnosis of the resected material yielded a neuroendocrine carcinoma; a hemangioma 1 cm in size was also found in the resected material.

Comments: Neuroendocrine tumors in the liver are usually metastases. It is not always possible to identify the localization of the extrahepatic primary tumor in the staging process. There were also no indications of an extrahepatic neuroendocrine tumor in this patient based on preoperative positron emission tomography using DOTA-TATE or on follow-up for 5 years after the resection.

7 Pseudotumors

The term hepatic pseudotumors is used to describe an intrahepatic region which appears to be a focal liver lesion due to a circumscribed change in echogenicity, but does not actually represent any form of neoplasm. The most common forms of pseudotumors are focal fat lesions or anatomical structures that mimic focal liver lesions:

– Focal fat lesions (fatty sparing, focal steatosis)

– Hypoechoic caudate lobe

– Pressure grooves from atrophied diaphragm (Zahn's grooves)

Focal fat lesions

A heterogeneous texture of the liver parenchyma may be due to focal fatty deposits or focal fatty sparing, which can mimic tumors and require a thorough diagnostic workup. Focal fatty liver is observed in patients with metabolic disorders (such as diabetes mellitus, obesity, alcohol abuse, porphyria), taking chemotherapy or hormone therapy, and with hepatic vascular pathologies. Focal fatty liver lesions are frequently observed around blood vessels or the gallbladder. These are dynamic over time, and can change with improved control of diabetes or with abstinence from alcohol. Zonal fat deposits have some typical characteristics in ultrasound (shape, localization, structure). When in doubt, contrast-enhanced ultrasound should be the primary method used to determine malignancy if a tumor is suspected (to exclude malignancy). Zonal fat depositions are identically isoenhanced as the surrounding tissue in contrast-enhanced ultrasound, whereas metastases in the parenchymal (late) phase are hypoenhanced (Table 5). If biopsies are taken in inconclusive cases, regions of heterogeneous echogenicity should be aspirated. Ideally, it should be possible to differentiate between increased or reduced fat deposition by histology.

Sonographic characteristics of fat depositions and fatty sparing
Localization – Anterior to portal vein/portal vein bifurcation – Gallbladder fossa – Subcapsular (rare)
Shape – Triangular/elongated – Segmented – Geographic – Well-defined margins
Vascular architecture remains intact
Echogenicity – Fatty sparing – Homogeneously hypoechoic – Fat deposition – Homogeneously hyperechoic
Contrast-enhanced ultrasound (CEUS) – Isoenhanced relative to surrounding liver tissue

Table 5

Focal fatty sparing

In the liver of patients with hepatic steatosis, circumscribed regions are observed which frequently exhibit no or much less fat. These regions are hypoechoic relative to the surrounding steatotic liver tissue and may mimic a tumor (pseudotumor). An experienced physician can diagnose this phenomenon by B-mode alone if the findings are typical. The most common localizations for focal fatty sparing are the region anterior to the portal vein and the gallbladder fossa (Fig. 70). Adjacent blood vessels are not misaligned, but rather frequently form anatomical borders. Hepatic veins are not displaced, but rather maintain their lengthy paths. This can be visualized particularly well using real-time imaging. In cases of fatty sparing in the more rare subcapsular localization, the contours of the liver remain intact, in contrast to tumors which may causes bulges in the capsule of the liver or may displace or infiltrate blood vessels. Contrasted-enhanced ultrasound may also be useful if tumors are suspected. Focal fatty sparing is enhanced by contrast identically to the surrounding tissue during the parenchymal phase, allowing metastases to be excluded.

Figure 70a and b: Focal fatty sparing anterior to the portal vein bifurcation.

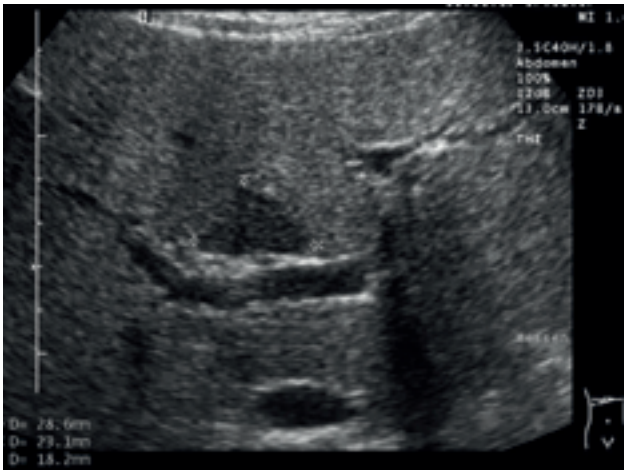

Figure 70a: Focal fatty sparing anterior to the portal vein bifurcation, triangular. Subcostal transverse view.

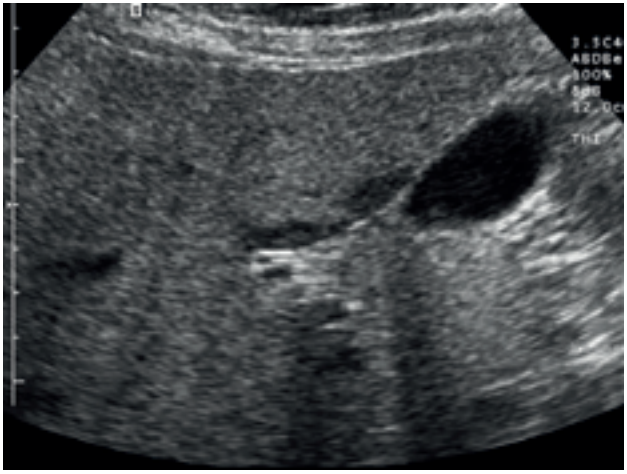

Figure 70b: Focal fatty sparing anterior to the portal vein bifurcation running along the interlobar fissure to the gallbladder.

Focal steatosis

Compared with the surrounding normal echogenic texture of the liver, focal steatosis is hyperechoic and well circumscribed, and is most frequently observed in the region around the branches of the portal vein and near the falciform ligament (Figs. 71–74). An experienced physician can diagnose this phenomenon by B-mode alone if the localization is typical and the patient has no history of cancer. Focal fat depositions can be differentiated from hemangioma by their location and by their usual oval or striated shape and occasional irregular contour. Focal steatosis may be observed in all liver segments. This makes a differential diagnosis between focal steatosis and fatty neoplasms (lipoma, angiomyolipoma, metastatic neuroendocrine tumors, fatty HCC) difficult at locations other than the typical steatosis location listed above. The most important feature that distinguishes steatosis from neoplasms is normal vascular architecture. Adjacent blood vessels are not misaligned, but rather frequently form anatomical borders. Contrast-enhanced ultrasound may prove helpful if B-mode imaging is inconclusive. Focal steatosis isoenhances with the liver parenchyma, allowing metastases to be excluded.

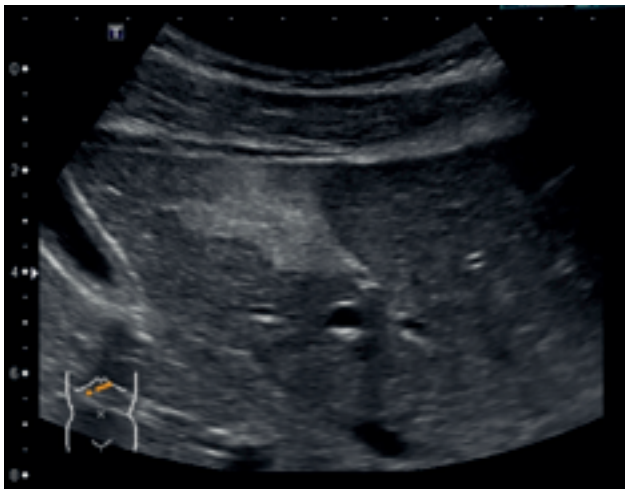

Figure 71: Focal steatosis near the falciform ligament (triangular configuration).

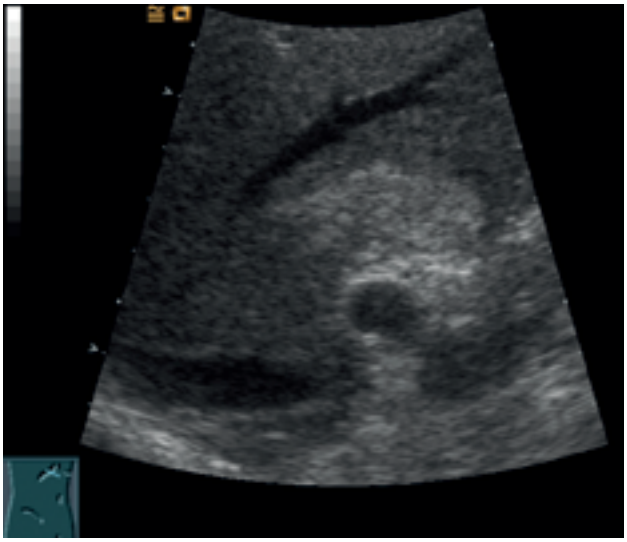

Figure 72: B-mode image of focal steatosis in the porta hepatis anterior to the portal vein.

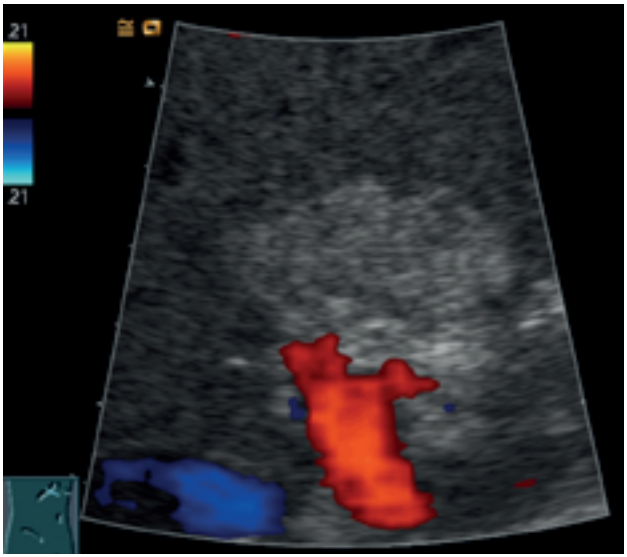

Figure 73: Color mode image of focal steatosis in the porta hepatis anterior to the portal vein.

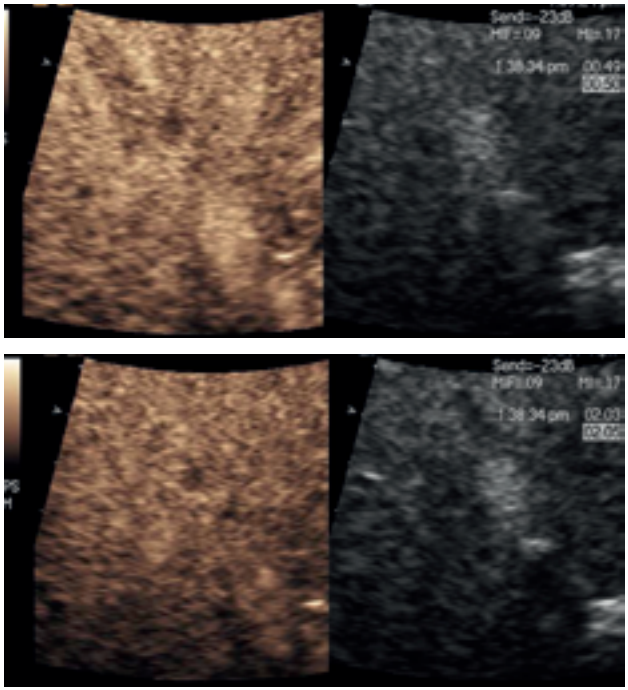

Figure 74: Focal steatosis in CEUS (50 s and 120 s p.i.). The hyperechoic mass appears isoenhanced.

Pitfall: Inflammatory pseudotumors

Pseudotumors are phenomena that appear to be focal tumor lesions, but are not. Table 6 provides an overview of phenomena detectable in ultrasound that may mimic focal liver lesions or malignant processes.

In patients with metabolic disorders, chemotherapy, or hormone therapy: – Heterogeneous fat depositions – Focal liver lesions due to Wilson's disease – α_1-Antitrypsin deficiency – Tyrosinemia type 1 – Gaucher's disease – Porphyria	**Vascular pathologies:** – Nodular regenerative hyperplasia due to Budd-Chiari syndrome (BCS) – Heterogeneous enlargement of the caudate lobe due to BCS – Pseudoaneurysm of the portal vein – Aneurysm of the hepatic arteries – Intrahepatic shunts – Focal liver lesions due to hereditary hemorrhagic telangiectasia – Geographic pathologies due to HELLP syndrome – Peliosis hepatis – Hepatic infarction (very rare)
Anatomical structures: – Round ligament of liver – Pressure grooves from the diaphragm (Zahn's grooves)	**Fibrosis/cirrhosis:** – Macronodular regenerative nodules – Focal confluent fibrosis – Bowed surface
Postoperative conditions, trauma: – Needle aspiration, endoscopy, spontaneous – Scar from cholecystectomy – Defects after resection – Clips – Pneumobilia – Seroma – Biloma – Hepatic portal venous gas – Hematoma/hemorrhage	**Bile duct pathologies:** – Hepatolithiasis – Caroli syndrome – Bile duct abscesses
Tumors: – Extrahepatic tumors	

Table 6: Differential diagnosis of pseudotumors.

Accessory lobes of liver and capsular retraction

Capsular retraction and accessory lobes of the liver are normal variations that may mimic a focal tumor lesion.

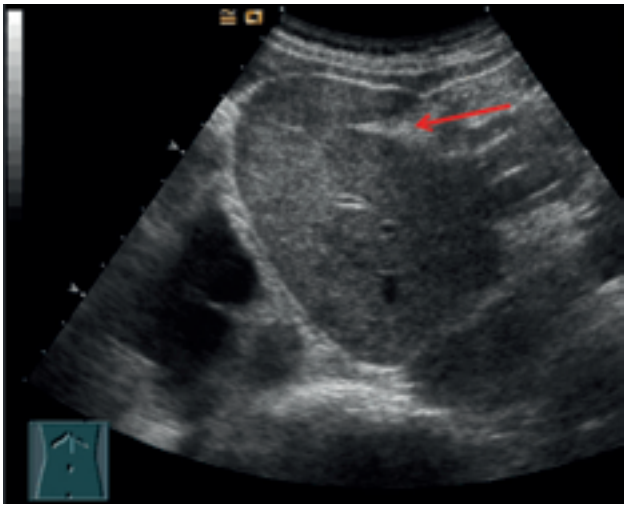

Figure 75: Transducer positioned longitudinally in the epigastric region, lower left lobe displayed: hyperechoic capsular retraction in the left lobe (arrow) and posterior accessory lobe formation.

Pressure grooves from the diaphragm (Zahn's grooves)

Pressure grooves from the diaphragm run along the diaphragmatic aspect of the right lobe of the liver. They result from the atrophy of muscle bundles in the diaphragm that leave striated impressions in the subdiaphragmatic region of the right lobe (Fig. 76). In a transverse ultrasound view, these pressure grooves appear as hyperechoic, striated or triangular regions which may be misinterpreted as hyperechoic masses if the angle of the transducer is unfavorable. There may be one or more of these pressure grooves. They are formed in patients with disorders such as pulmonary emphysema owing to the increased use of the respiratory muscles, or in well-trained athletes.

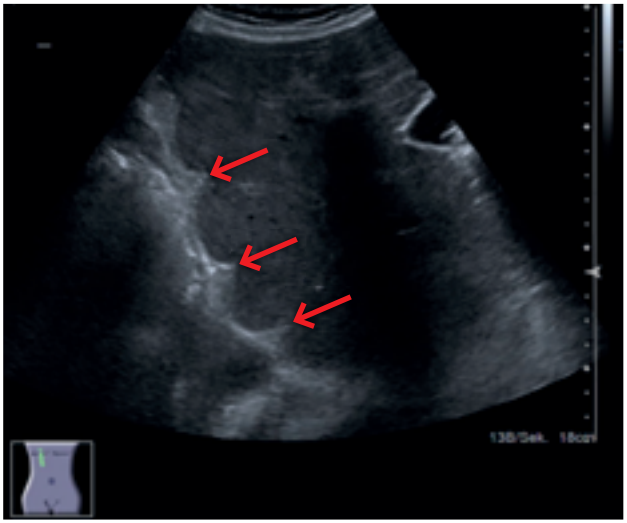

Figure 76: Pressure grooves from the diaphragm: intercostal transducer position. Multiple hyperechoic capsular retractions are visible in the posterior subdiaphragmatic region. Ultrasound allows these hyperechoic capsular retractions to be anatomically identified as belonging to the diaphragm based on their localization (posterior subdiaphragmatic) and their striated shape (arrows).

Falciform ligament

In the left lobe of the liver, the falciform ligament may be misinterpreted as hemangioma as it is a hyperechoic structure. The falciform ligament appears in a transverse view as a triangular form, and in a longitudinal view it appears as a striated, hyperechoic structure running in an anterior direction to the abdominal wall (Fig. 77). It separates liver segments III and IV.

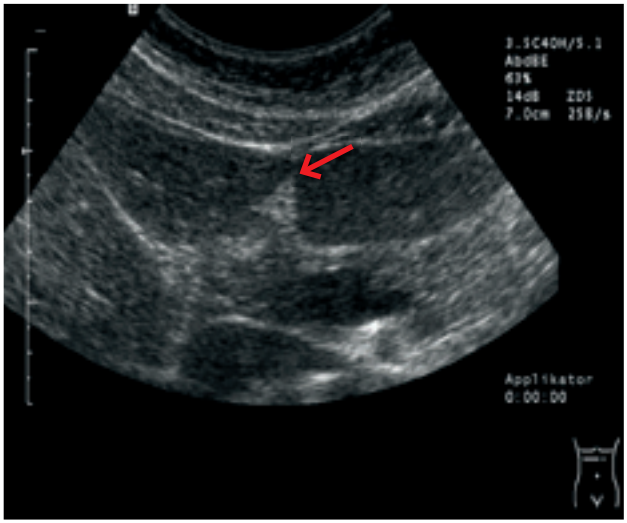

Figure 77: Falciform ligament (transverse view): Transducer on epigastric region (transverse view). The falciform ligament appears with a triangular shape (arrow). The interlobar fissure is visible on the left-hand side of the image.

Calcification

Calcification is occasionally observed in the liver, and can be differentiated from echogenic liver lesions by its posterior acoustic attenuation (Fig. 78). Calcification of this nature is also frequently found in other organs, especially the spleen. It typically results from past infections, for example tuberculosis. The differential diagnoses include pneumobilia (Fig. 79) or hepatolithiasis (Figs. 45 and 46) along the course of the hepatic bile ducts. Calcification can also occasionally be observed in focal liver lesions, for example in metastases that have regressed, in HCC lesions, or in the walls of hydatid cysts.

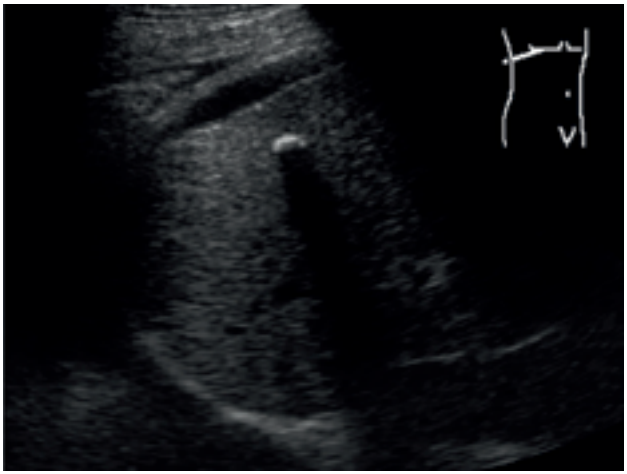

Figure 78: 1 cm calcification in subcapsular region of segment VII: hyperechoic bulging scatter with acoustic attenuation (secondary finding of subphrenic free fluid).

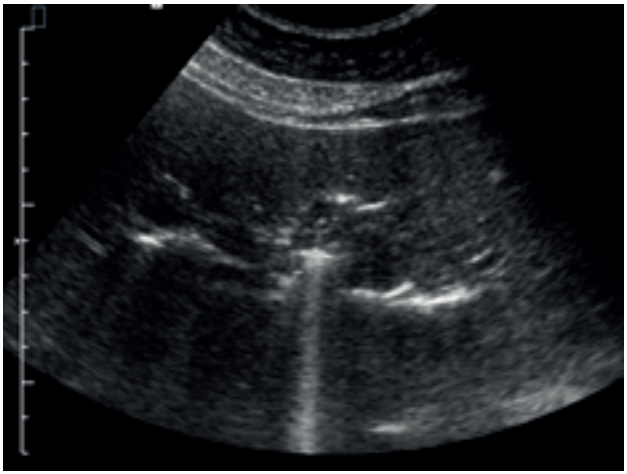

Figure 79: Pneumobilia (gas accumulation) in the bile ducts. In contrast to circumscribed calcification, the hyperechoic phenomena are elongated or strip-like, and follow the course of the intrahepatic bile ducts next to the portal veins. A reverberation artifact is visible in the center of the image. The movement of the gas bubbles upon a shift in patient position could also be detected by real-time imaging.

Porphyria cutanea tarda

Chronic hepatic porphyria appears as multiple, well circumscribed, hyperechoic liver lesions. A prominent hyperechoic rim is sometimes observed in B-mode imaging (Fig. 80). Contrast-enhanced ultrasound can help differentiate porphyria from hemangiomas or hyperechoic metastases: there is no peripheral nodular enhancement as is typical of hemangioma, or hypoenhancement in the portal venous and late phases as is typical of malignancies (Fig. 81). The urinary detection of porphyrin metabolites can confirm the diagnosis. The hyperechoic liver lesions represent focal steatosis with no impact on vascular architecture. If a biopsy is performed, histology can confirm steatosis with lobular infiltration by Kupffer cells and hemosiderin deposition.

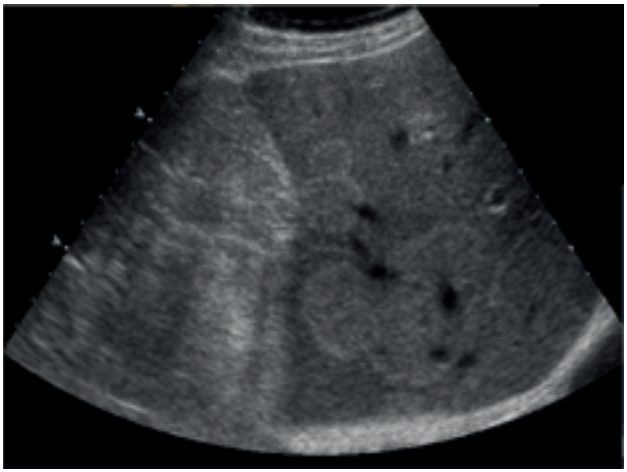

Figure 80: B-mode image of focal steatosis due to porphyria cutanea tarda: multiple hyperechoic, well circumscribed lesions with prominent margins appear in the right lobe with no impacts on the vascular architecture or the contours of the liver.

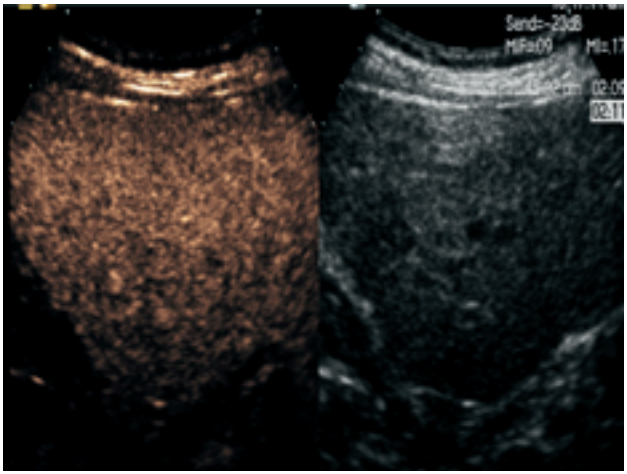

Figure 81: CEUS: focal steatosis due to porphyria cutanea tarda. The lesions are isoenhanced in contrast-enhanced ultrasound.

8 Focal nodular hyperplasia

Focal nodular hyperplasia (FNH) is the second-most frequent form of benign solid focal liver lesion, and affects women at a much higher rate than men. Both the incidence and the prevalence of the disorder are increasing, most likely as a result of the increasing use of diagnostic imaging procedures. The typical age of first diagnosis in women is 20–50 years old. In men, FNH is associated with the use of anabolic steroids. FNH is not an actual neoplasm, but rather is most likely the consequence of an arteriovenous malformation resulting from progressive, regional nodular hyperplasia of liver tissue.

FNH is typically discovered by ultrasound as an incidental finding or when attempting to elucidate elevated levels of gamma-glutamyltransferase (GGT) or alkaline phosphatase (AP). Higher levels of GGT and AP are most often observed with larger FNH (> 5 cm) and can be explained by proliferation into the bile ducts.

B-mode findings: In a healthy, not steatotic liver, FNH has a liver-like appearance (hyperplasia); however, it is not possible to confirm a diagnosis of FNH by B-mode ultrasound. Smaller lesions are typically homogeneous, while a hyperechoic stellate scar can be observed in typical FNH lesions which are 3 cm or larger. The radiating fibrous septa contain arteries that are responsible for the characteristic spoke-wheel pattern observed in color Doppler ultrasound (Fig. 82a) or in power mode (Fig. 82b). Low arterial resistance is typical with FNH. The spectra observed in pulsed-wave (PW) Doppler mode appear similar to those of an arteriovenous fistula with a high share of diastolic flow. The resistance index (RI) is usually low (RI < 0.5).

Figure 82a and b: Focal nodular hyperplasia: typical spoke-wheel pattern in power mode and color mode.

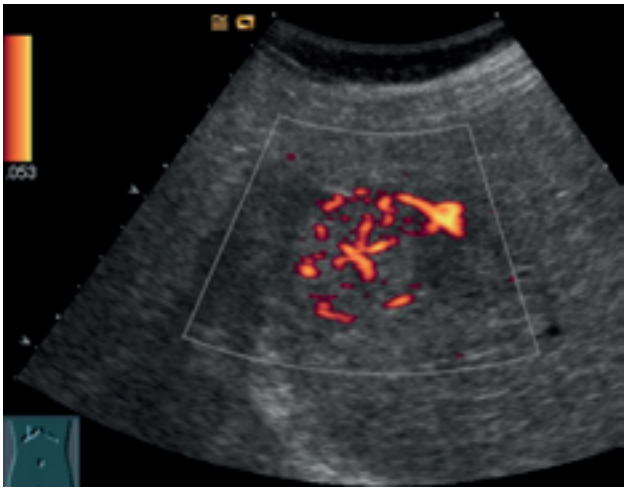

Figure 82a: FNH: Spoke-wheel pattern in power mode.

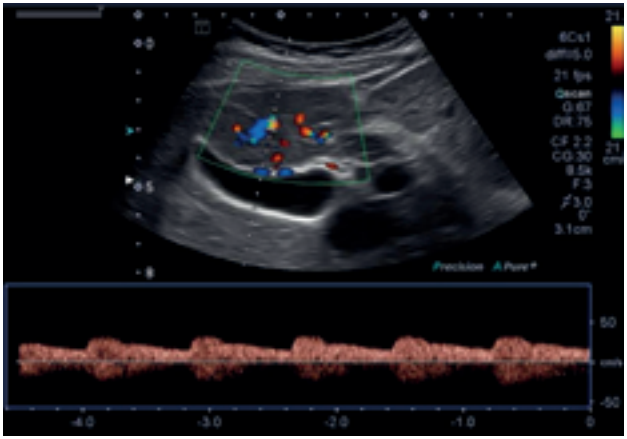

Figure 82b: FNH in color mode and PW Doppler (arterial flow profile with low RI).

FNH in color mode and contrast-enhanced ultrasound

Two primary types of FNH can be differentiated by color Doppler or contrast-enhanced ultrasound:

– the more common "classical" FNH with a prominent central artery and spoke-like branching of arteries in fibrous septa, and

– the less common telangiectatic form of FNH without a central stellate scar (= inflammatory adenoma).

The latter form is characterized by thickened vessels and dilated sinusoids, and contains less fibrosis. The telangiectatic form of FNH has now been reclassified as an inflammatory adenoma based on recent molecular pathology studies (see section on adenomas). In addition to the classical and telangiectatic forms of FNH, there are several other variants that are difficult to differentiate from adenomas, nodular regenerative hyperplasia, or multiacinar regenerative nodules [Wermke 2006]. In the majority of classical FNH lesion (85%), the diagnosis can be confirmed by contrast-enhanced ultrasound [Strobel et al. 2009]. If there are any doubts about classification (atypical enhancement, scar absent, calcification), a second imaging modality should be used, preferably MRI with a liver-specific contrast agent. Should the findings remain inconclusive, histological confirmation is recommended. Ultrasound-guided needle biopsy expedites the diagnostic procedure, and is usually performed to differentiate FNH from adenoma. Cases of asymptomatic FNH should be monitored. An increase in the size of FNH during pregnancy is quite rare, and case series of pregnant women have not reported any complications of FNH [Rifai et al. 2013]. Malignant transformation of FNH has not been described [Bennett & Bova 1990; Wermke 2006]. A biopsy is not required if there is clear evidence of FNH in CEUS.

The typical contrast behavior of FNH in CEUS is a very rapid uptake of contrast during the early arterial phase, well before the enhancement of the liver in the arterial phase. In classical FNH, this enhancement has a centrifugal spoke-like dynamic (Fig. 83), while the telangiectatic form displays a centripetal pattern filling from the rim inwards without any spokes. The dilated arterial lumens found in large classical FNH may exhibit a type of "steal phenomenon", in which contrast fills the FNH through the dilated arteries very rapidly during the arterial phase, even prior to enhancement of the surrounding liver tissue.

Both forms of FNH are enhanced more intensely than the surrounding liver tissue during the arterial phase, and this greater enhancement often persists into the portal venous phase. During the late phase, the enhancement of the FNH is equivalent to that of the surrounding liver tissue (isoenhancement). FNH can be differentiated from metastases based on isoenhancement or hyperenhancement in the late phase (Fig. 84).

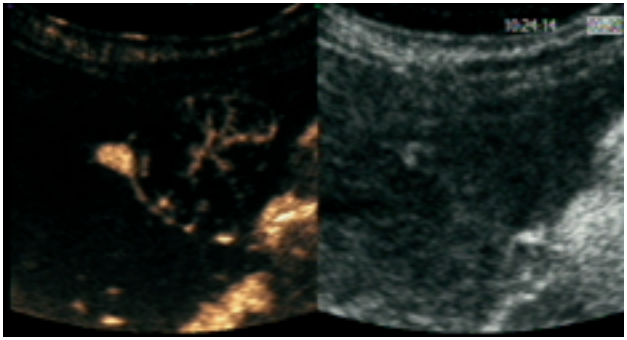

Figure 83: FNH in contrast-enhanced ultrasound: typical spoke-wheel pattern in the early arterial phase.

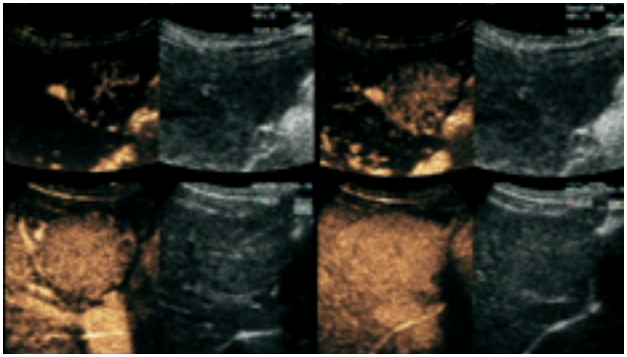

Figure 84: FNH in contrast-enhanced ultrasound. Spoke-wheel pattern and rapid enhancement in the arterial phase (before enhancement of surrounding liver tissue during the arterial phase, isoenhancement to hyperenhancement during the portal venous phase extending into the late phase [2:08]: hyperenhanced lesion, punctate central hypoenhancement [central scar]).

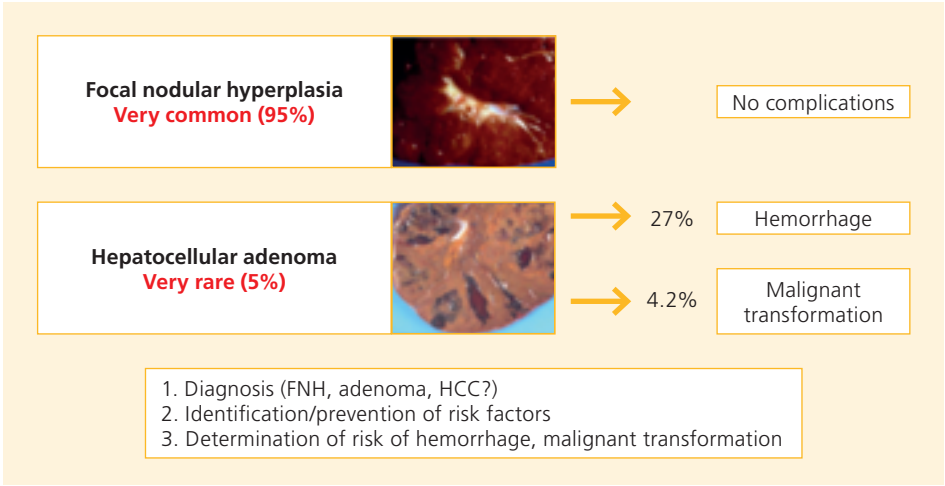

Figure 85: Differential diagnosis of FNH and hepatocellular adenoma.

9 Hepatocellular adenoma

Hepatocellular adenomas (HCA) are rare neoplasms that are usually benign, and which are located by definition in a non-cirrhotic liver. HCA are observed most frequently in women who have taken oral contraceptives for many years. However, glycogen storage disease, obesity, cardiovascular disorders, use of anabolic steroid hormones, and alcohol abuse also all represent risk factors for HCA in both women and men [Bieze et al. 2014].

Hepatocellular adenoma represents a heterogeneous entity. The most common subtypes are HNF-1α-inactivated hepatocellular adenoma (H-HCA) and inflammatory hepatocellular adenoma (I-HCA), which together comprise about 80% of all cases. Much less common are the β-catenin-activated subtype (β-catenin HCA) and the subtype of unclassified HCA (Bordeaux classification; Fig. 86). Classifying the subtype of HCA can provide additional information about a patient's prognosis and indicated therapy [Nault et al. 2012, 2013]. A biopsy is usually required to confirm the adenoma subtype. Cases of more than 10 adenomas in one patient are termed liver adenomatosis. This condition is very rare with an approximately equal incidence between genders, and may be triggered by abuse of anabolic steroids.

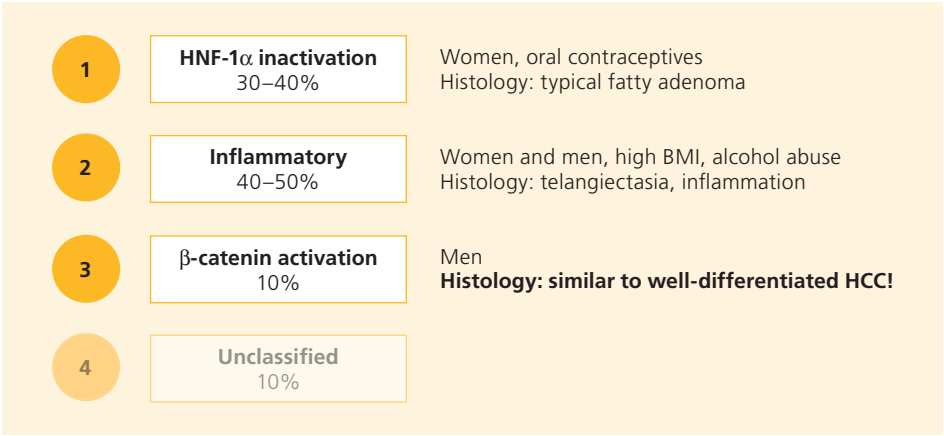

Figure 86: Classification of hepatocellular adenoma [Bioulac-Sage et al. 2011].

The morphology of HCA in ultrasound is variable and does not aid in diagnosis. The appearance of HCA varies by its fat content among other factors. In contrast-enhanced ultrasound, inflammatory adenoma is characterized by a very rapid uptake of contrast agent faster than the surrounding liver tissue (pooling), with enhancement proceeding from the margin to the center. Unlike FNH, there is no central artery and no spoke-wheel pattern of contrast enhancement. Inflammatory adenoma (previously called telangiectatic FNH) is characterized by isoenhancement or even hyperenhancement into the late phase (Figs. 87 and 88), as the dilation of the sinusoids prevents rapid wash-out of the contrast agent. Liver MRI using liver-specific contrast agents is recommended for inconclusive cases.

The classical form of fatty adenoma (H-HCA) can be characterized by MRI due to its fat content. Both contrast-enhanced ultrasound and liver MRI can detect hemorrhage, which can occur in H-HCA based on the size of the lesion.

For the majority of (typically female) patients, a non-invasive diagnosis of a hepatocellular adenoma (inflammatory adenoma and fatty adenoma) is possible using the combination of contrast-enhanced ultrasound and liver MRI (with liver-specific contrast agents). A CT scan of the liver is of little diagnostic value. Should it not be possible to confirm a diagnosis by contrast-enhanced ultrasound and liver MRI, or if there is a potential differential diagnosis of HCC based on the clinical particulars (male patient, age > 50 years, metabolic syndrome, known parenchymal liver disease), an ultrasound-guided liver biopsy or resection of the lesion should be performed.

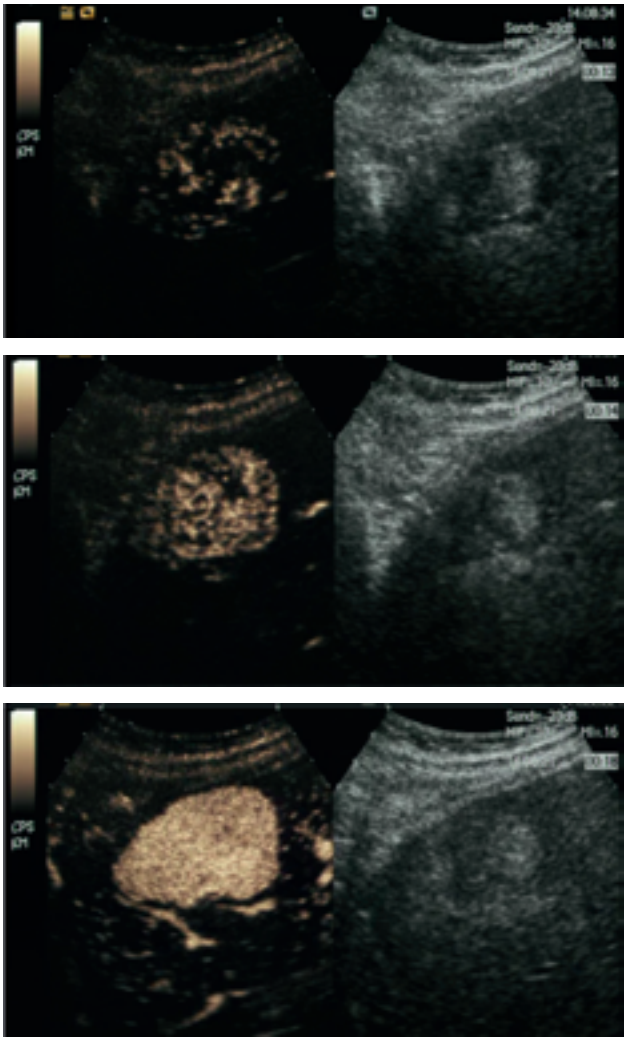

Figure 87: Hepatocellular adenoma (inflammatory subtype). Contrast enhancement during the early arterial/arterial phase: very rapid uptake of contrast agent (CEUS 13 s, 14 s, and 18 s) faster than the surrounding liver tissue (pooling) with centripetal enhancement.

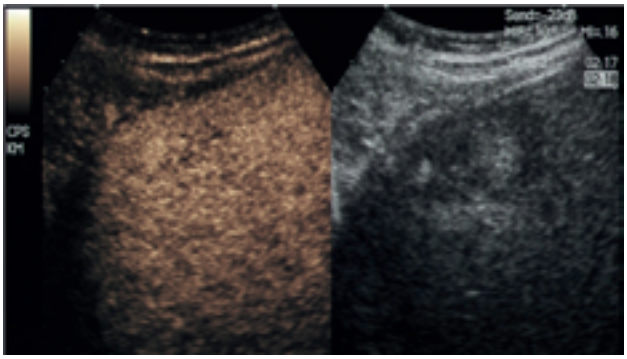

Figure 88: Hepatocellular adenoma (inflammatory subtype): the adenoma exhibits isoenhancement during the late phase after 2 and 3 minutes of CEUS.

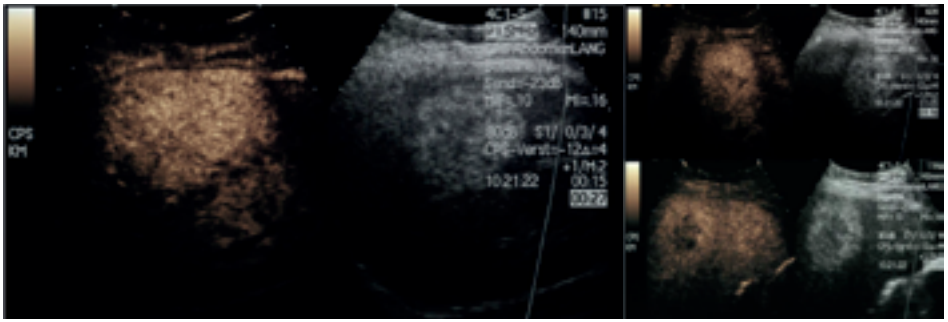

Figure 89: Hepatocellular adenoma (H-HCA subtype) in contrast-enhanced ultrasound: arterial phase (27 s p.i.) isoenhanced, portal venous phase (76 s p.i.) isoenhanced, late phase (137 s p.i.) centrally hypoenhanced. The histology of classical fatty adenoma (H-HCA) is characterized by an increased fat content. In this example, the fat content could also be detected by hyperechogenicity in B-mode.

It was previously thought that all cases of hepatocellular adenoma should be resected; however, this is no longer the case. Rather, the risks associated with HCA (hemorrhage, malignant transformation) should first be weighed before making a case-by-case recommendation for surgical removal.

The risk of hemorrhage – which depends on the size of the lesion – is 29%, and is thus actually much greater than the risk of malignant transformation at 4.2% [Cho et al. 2008; Stoot et al. 2010].

Factors associated with a markedly higher risk of HCA hemorrhage are lesion size > 5 cm, subcapsular localization, and pregnancy. Surgical resection should be recommended to patients with any of these risk factors even if they are asymptomatic [Bieze et al. 2014]. Should patients decline or be ineligible for surgery, the size of the lesion should be monitored by ultrasound (including CEUS if needed) in order to detect potential hemorrhage. There are case series in the literature describing local ablation procedures (transarterial embolization, radiofrequency embolization).

The risk of malignant transformation of HCA has traditionally been overestimated [Dokmak et al. 2009; Farges et al. 2011]. Malignant transformation of HNF1α-inactivated HCA or inflammatory adenoma occurs extremely rarely, and hence monitoring the size of the lesion and the patient's clinical symptoms is sufficient for asymptomatic patients and for lesions < 5 cm in size. β-catenin-activated HCA is a unique case among the forms of HCA. HCA with mutated β-catenin poses a greater risk of malignant transformation, and is also the most common subtype of HCA in men. It is necessary to histologically confirm the diagnosis and subtype of an HCA in order to classify it as β-catenin-activated HCA. Due to the greater risk of malignant transformation, β-catenin-activated HCA should be resected regardless of its size [Goltz et al. 2015].

10 Case reviews of rare benign liver nodules

The differential diagnoses of hemangioendothelioma, bile duct adenoma, lipoma, angiolipoma, myeloylipoma, and angiomyolipoma need to be considered for liver nodules of unknown origin. Although biliary hamartomas are very frequently discovered by pathologists when performing autopsies, they are frequently not detected by imaging techniques as they are typically only a few millimeters in size.

Biliary hamartoma

Biliary hamartomas, or von Meyenburg complexes, are benign hamartomas that originate from intrahepatic bile ducts (congenital bile duct malformation, cholangioma) and are comprised of fibrous stroma and cysts covered with biliary epithelium. They may be solitary or multifocal, and are so small (0.5–15 mm) that they are usually not detectable by imaging modalities. These forms of cholangioma appear in ultrasound as hyperechoic nodules with or without polycystic degeneration (Fig. 90) [Krahn et al. 2012].

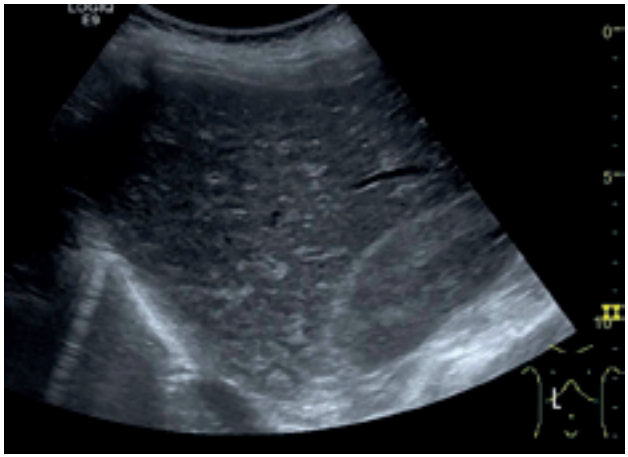

Figure 90: Biliary hamartomas.

Angiomyolipoma

Case review: 65-year-old man with chronic hepatitis C. Hemangioma was diagnosed by ultrasound. The lesion was resected (MRI findings were not typical of hemangioma). The liver was not cirrhotic. Angiomyolipoma and hemangioma cannot be differentiated in B-mode imaging (Figs. 91 and 92).

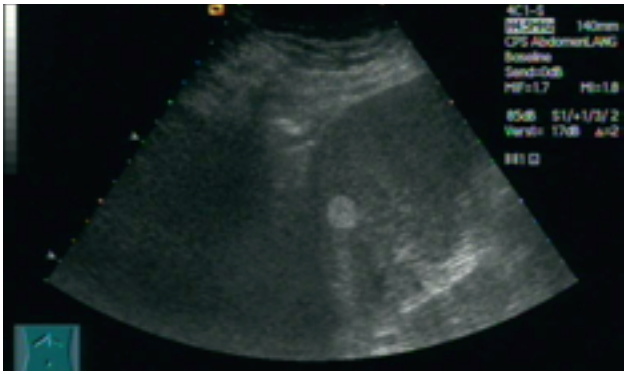

Figure 91: Angiomyolipoma confirmed by histology in a 65-year-old man with hepatitis C (overview).

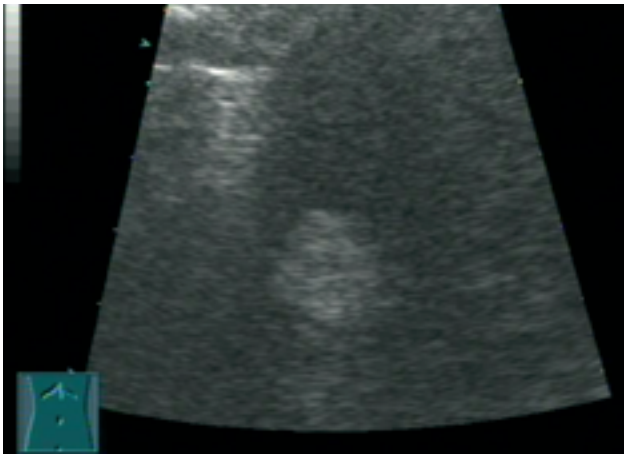

Figure 92: Zoom mode.

Cholangioma

Case review: Incidental finding in a 74-year-old man; diabetes mellitus, no known prior malignancies, metabolic syndrome.

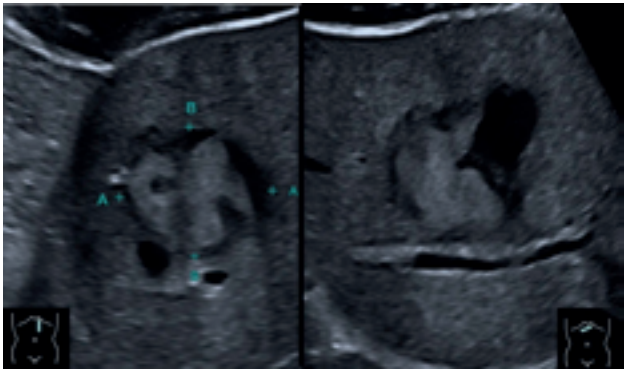

Figure 93: Cholangioma confirmed by biopsy (B-mode). 3 cm lesion with a solid and a cystic component with no vascularity in color Doppler.

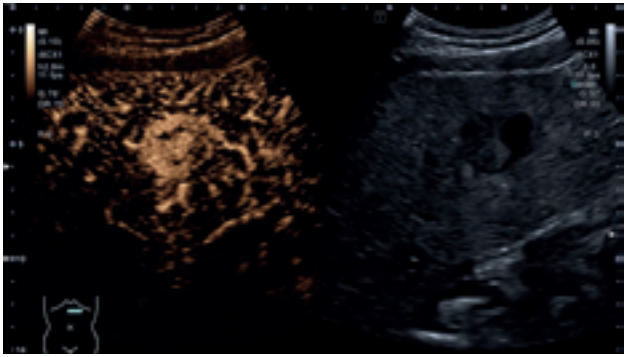

Figure 94: Cholangioma confirmed by biopsy (contrast-enhanced ultrasound). The lesion was revealed to be completely hypervascular at 19 s after administration of contrast agent. Surprisingly, the anechoic component also became enhanced (was suspected to be cystic by B-mode) somewhat later in the portal phase.

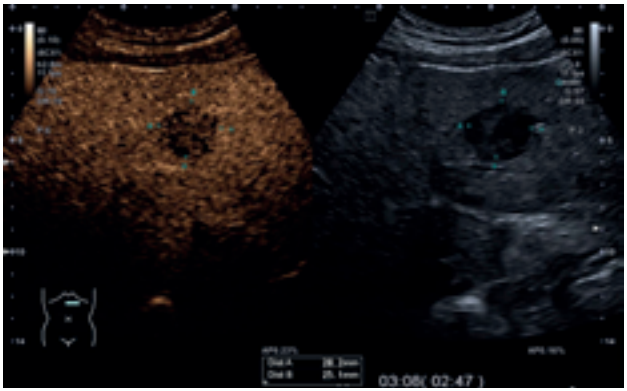

Figure 95: Cholangioma confirmed by biopsy (contrast-enhanced ultrasound). In the late phase (almost 3 min p.i.), the lesion is hypoenhanced relative to the surrounding liver tissue, and is thus suspected to be malignant.

Ultrasound-guided needle biopsy was performed on the solid component of the lesion and the surrounding liver tissue. The biopsy of the lesion revealed a cholangioma, while the histology of the liver parenchyma revealed hepatic steatosis.

Based on the hypoenhancement during the late phase (suspected malignancy), the patient continued to be monitored closely by ultrasound for changes of the size despite the biopsy of the lesion being classified as benign. When the size of the lesion grew slightly after 6 weeks, a recommendation was made for surgical removal with the patient's consent. Histology of the resected material revealed a cholangiocarcinoma 3 cm in size (G2).

Remember: A liver lesion that is hypoenhanced during the late phase of contrast-enhanced ultrasound is always highly suspicious of being malignant. A plausibility check should also be performed on all biopsy results in routine clinical practice. It is necessary to perform a re-biopsy, or at least to monitor changes in the size of the lesion over time in ultrasound for lesions with conflicting findings (suspected malignancy in contrast-enhanced ultrasound but benign in biopsy).

11 Literature

Bennett WF, Bova JG. Review of hepatic imaging and a problem-oriented approach to liver masses. Hepatology. 1990;12(4 Pt 1):761–75.

Bieze M, Phoa SS, Verheij J, van Lienden KP, van Gulik TM. Risk factors for bleeding in hepatocellular adenoma. Br J Surg. 2014;101(7):847–55.

Bioulac-Sage P, Cubel G, Balabaud C, Zucman-Rossi J. Revisiting the pathology of resected benign hepatocellular nodules using new immunohistochemical markers. Semin Liver Dis. 2011;31(1):91–103.

Brunetti E, Kern P, Vuitton DA; Writing Panel for the WHO-IWGE. Expert consensus for the diagnosis and treatment of cystic and alveolar echinococcosis in humans. Acta Trop. 2010;114(1):1–16.

Cho SW, Marsh JW, Steel J, Holloway SE, Heckman JT, Ochoa ER, et al. Surgical management of hepatocellular adenoma: take it or leave it? Ann Surg Oncol. 2008;15(10):2795–803.

Claudon M, Dietrich CF, Choi BI, Cosgrove DO, Kudo M, Nolsøe CP, et al. Guidelines and good clinical practice recommendations for contrast enhanced ultrasound (CEUS) in the liver – update 2012: a WFUMB-EFSUMB initiative in cooperation with representatives of AFSUMB, AIUM, ASUM, FLAUS and ICUS. Ultraschall Med. 2013;34(1):11–29.

Corvino A, Catalano O, Corvino F, Sandomenico F, Petrillo A. Diagnostic Performance and Confidence of Contrast-Enhanced Ultrasound in the Differential Diagnosis of Cystic and Cystic-like Liver Lesions. Am J Roentgenol. 2017;209(3):W119–W127.

Dokmak S, Paradis V, Vilgrain V, Sauvanet A, Farges O, Valla D, et al. A single-center surgical experience of 122 patients with single and multiple hepatocellular adenomas. Gastroenterology. 2009;137(5):1698–705.

Dong Y, Wang WP, Mao F, Fan M, Ignee A, Serra C, et al. Contrast enhanced ultrasound features of hepatic cystadenoma and hepatic cystadenocarcinoma. Scand J Gastroenterol. 2017;52(3):365–72.

Farges O, Ferreira N, Dokmak S, Belghiti J, Bedossa P, Paradis V. Changing trends in malignant transformation of hepatocellular adenoma. Gut. 2011;60(1):85–9.

Goltz D, Fischer HP. Hepatozelluläre Tumoren im nichtzirrhotischen Lebergewebe. Pathologe. 2015;36(6):597–606.

Kaltenbach TE, Engler P, Kratzer W, Oeztuerk S, Seufferlein T, Haenle MM, et al. Prevalence of benign focal liver lesions: ultrasound investigation of 45,319 hospital patients. Abdom Radiol (NY). 2016;41(1):25–32.

Karhunen PJ. Benign hepatic tumours and tumour like conditions in men. J Clin Pathol 1986;39(2):183–8.

Kasper HU, Drebber U, Dries V, Dienes HP. Lebermetastasen: Inzidenz und histogenetische Einordnung. Z Gastroenterol 2005;43(10):1149–57.

Krahn JF, Bönhof JA, Förster C, Eckardt AJ. Von Meyenburg complexes: a rare cause for multiple hepatic lesions on transabdominal ultrasound. J Clin Ultrasound. 2012;40(3):174–5.

Kratzer W, Gruener B, Kaltenbach TE, Ansari-Bitzenberger S, Kern P, Fuchs M, et al. Proposal of an ultrasonographic classification for hepatic alveolar echinococcosis: Echinococcosis multilocularis Ulm classification-ultrasound. World J Gastroenterol. 2015;21(43):12392–402.

Kunze G, Staritz M, Köhler M.Contrast-enhanced ultrasound in different stages of pyogenic liver abscess. Ultrasound Med Biol. 2015;41(4):952–9.

McManus DP, Zhang W, Li J, Bartley PB. Echinococcosis. Lancet. 2003;362(9392):1295–304.

Nault JC, Fabre M, Couchy G, Pilati C, Jeannot E, Tran Van Nhieu J, et al. GNAS-activating mutations define a rare subgroup of inflammatory liver tumors characterized by STAT3 activation. J Hepatol. 2012;56(1):184–91.

Nault JC, Bioulac-Sage P, Zucman-Rossi J. Hepatocellular benign tumors-from molecular classification to personalized clinical care. Gastroenterology. 2013;144(5):888–902.

Piscaglia F, Nolsøe C, Dietrich CF, Cosgrove DO, Gilja OH, Bachmann Nielsen M, et al. The EFSUMB Guidelines and Recommendations on the Clinical Practice of Contrast Enhanced Ultrasound (CEUS): update 2011 on non-hepatic applications. Ultraschall Med. 2012;33(1):33–59.

Rifai K, Mix H, Krusche S, Potthoff A, Manns MP, Gebel MJ. No evidence of substantial growth progression or complications of large focal nodular hyperplasia during pregnancy. Scand J Gastroenterol. 2013;48(1):88–92.

Rübenthaler J, Mueller-Peltzer M, Negrão de Figueiredo G, Gresser E, Clevert DA. CEUS – Diagnostik zystischer Nierenläsionen. Radiologe. 2018;58(6):545–52.

Seitz K, Greis C, Schuler A, Bernatik T, Blank W, Dietrich CF, et al. Frequency of tumor entities among liver tumors of unclear etiology initially detected by sonography in the noncirrhotic or cirrhotic livers of 1349 patients. Results of the DEGUM multicenter study. Ultraschall Med. 2011;32(6):598–603.

Stoot JH, Coelen RJ, De Jong MC, Dejong CH. Malignant transformation of hepatocellular adenomas into hepatocellular carcinomas: a systematic review including more than 1600 adenoma cases. HPB (Oxford). 2010;12(8):509–22.

Strobel D, Seitz K, Blank W, Schuler A, Dietrich C, von Herbay A, et al. Contrast-enhanced ultrasound for the characterization of focal liver lesions – diagnostic accuracy in clinical practice (DEGUM multicenter trial). Ultraschall Med. 2008;29(5):499–505.

Strobel D, Seitz K, Blank W, Schuler A, Dietrich CF, von Herbay A, et al. Tumor-specific vascularization pattern of liver metastasis, hepatocellular carcinoma, hemangioma and focal nodular hyperplasia in the differential diagnosis of 1,349 liver lesions in contrast-enhanced ultrasound (CEUS). Ultraschall Med. 2009;30(4):376–82.

Tang C, Fang K, Guo Y, Li R, Fan X, Chen P, et al. Safety of Sulfur Hexafluoride Microbubbles in Sonography of Abdominal and Superficial Organs: Retrospective Analysis of 30,222 Cases. J Ultrasound Med. 2017;36(3):531–8.

Thomeer MG, Broker M, Verheij J, Doukas M, Terkivatan T, Bijdevaate D, et al. Hepatocellular adenoma: when and how to treat? Update of current evidence. Therap Adv Gastroenterol. 2016;9(6):898–912.

Wermke W. Sonographische Differenzialdiagnose – Leberkrankheiten. Lehrbuch und systematischer Atlas. Köln: Deutscher Ärzte-Verlag. 2006.

Wildner D, Bernatik T, Greis C, Seitz K, Neurath MF, Strobel D. CEUS in hepatocellular carcinoma and intrahepatic cholangiocellular carcinoma in 320 patients – early or late washout matters: a subanalysis of the DEGUM multicenter trial. Ultraschall Med. 2015;36(2):132–9.

FALK FOUNDATION e.V.

Leinenweberstr. 5
79108 Freiburg
Germany

U42-1e 1-1/2020 POP